Structural and Chemical Properties of Zwitterionic Iridium Complexes Featuring the Tripodal Phosphine Ligand $[PhB(CH_2PPh_2)_3]^-$

Jay D. Feldman, Jonas C. Peters,† and T. Don Tilley*

Department of Chemistry, University of California at Berkeley, Berkeley, California 94720-1460

Received June 26, 2002

Several new iridium compounds bearing the $PhB(CH_2PPh_2)_3^-$ (herein abbreviated as $[PhBP_3]$) ligand have been prepared and characterized, and a comparison of steric, electronic, and chemical properties is made with those of related pentamethylcyclopentadienyl (Cp*) and hydridotris(3,5-dimethylpyrazolyl)borate (Tp^{Me_2}) complexes. The complexes $[PhBP_3]Ir(H)(\eta^3\text{-}C_8H_{13})$ (**2**) and $[PhBP_3]Ir(H)(\eta^3\text{-}C_3H_5)$ (**3**) were synthesized from the reaction of $[Li(TMED)][PhBP_3]$ (**1**) with the corresponding $[(alkene)_2IrCl]_2$ complex. These allyl complexes serve as precursors to the dihalides $[PhBP_3]IrX_2$ (**10**, X = I; **12**, X = Cl). In addition to these dihalides, the five-coordinate species $[PhBP_3]IrMe_2$ (**16**) and $[ClB(CH_2PPh_2)_3]IrCl_2$ (**13**) have been isolated. Addition of CO to **2** or **3** gave $[PhBP_3]Ir(CO)_2$ (**7**), while reaction of H_2 with **2** yielded $\{[PhBP_3]IrH_2\}_2$ (**8**) in benzene and $[PhBP_3]Ir(COE)H_2$ (**9**) in THF (where COE = cyclooctene). Complex **2** reacted with $PMePh_2$ to give $[PhBP_3]Ir(PMePh_2)H_2$ (**5**) and 1,3-cyclooctadiene. The protonation of **5** with $[H(OEt_2)]\{B[3,5\text{-}C_6H_3(CF_3)_2]_4\}$ gave the classical hydride complex $\{[PhBP_3]Ir(PMePh_2)H_3\}\{B[3,5\text{-}C_6H_3(CF_3)_2]_4\}$ (**6**). In addition to the formation of allyl complexes **2** and **3**, several C−H activation reactions have been observed; addition of PMe_3 to **2** provided the cyclometalated product $\{PhB[(CH_2PPh_2)_2(CH_2PPhC_6H_4)]\}Ir(H)(PMe_3)$ (**4**) and COE. Photolysis of **5** gave $\{PhB[(CH_2PPh_2)_2(CH_2PPhC_6H_4)]\}Ir(H)(PMePh_2)$ (**A**) and $[PhBP_3]Ir(H)(PMePhC_6H_4)$ (**B**). Complex **9** catalyzes H/D exchange between COE and benzene-d_6. Metathesis reactions of diiodide **10** with $LiBHEt_3$ gave $[Li(THF)_n]\{[PhBP_3]Ir(H)_2I\}$ (**14a**) and $[Li(THF)_n]\{[PhBP_3]Ir(H)_3\}$ (**15**). Comparison of the spectroscopic properties of related $[PhBP_3]Ir$, Cp*Ir, and $Tp^{Me_2}Ir$ complexes suggests that relative donating abilities follow the trend $[PhBP_3] \geq Cp^* > Tp^{Me_2}$, and structural comparisons indicate that $[PhBP_3]$ is the most sterically demanding ligand.

Introduction

Advances in transition-metal chemistry are to a large extent paced by the design and synthesis of new types of ligands which influence the properties and reactivity of a metal center. Currently, there is significant interest in anionic six-electron donors such as cyclopentadienyl (Cp), pentamethylcyclopentadienyl (Cp*), hydridotris(pyrazolyl)borate (Tp), and hydridotris(3,5-dimethylpyrazolyl)borate (Tp^{Me_2}). Transition-metal complexes featuring these ligands are common in organometallic chemistry and exhibit a rich variety of interesting catalytic and stoichiometric reactions. Despite the isoelectronic relationship between these ligands, they differ significantly; for example, Cp* is a relatively soft ligand which coordinates with its π-system, while Tp^{Me_2} has relatively hard nitrogen σ-donors.[1] Such factors are likely responsible for the differences in properties and reactivities observed for analogous Tp^{Me_2} and Cp* complexes.[1−8]

Recent reports have described a new type of anionic six-electron ligand based on phosphorus donors, $PhB(CH_2PPh_2)_3^-$ (herein abbreviated as $[PhBP_3]$).[9,10] Related sulfur-based ligands, $PhB(CH_2SR)_3^-$, have been developed by Riordan and co-workers.[11] In some ways, $[PhBP_3]$ would seem to possess properties that are intermediate between those of Tp ligands and Cp ligands. For $[PhBP_3]$ the phosphorus donor atoms are soft, like the π-system of Cp ligands, yet $[PhBP_3]$

† Current address: Division of Chemistry and Chemical Engineering, California Institute of Technology, Pasadena, CA 91125.

(1) Trofimenko, S. *Chem. Rev.* **1993**, *93*, 943−980.
(2) Tellers, D. M.; Skoog, S. J.; Bergman, R. G.; Gunnoe, T. B.; Harman, W. D. *Organometallics* **2000**, *19*, 2428−2432.
(3) Tellers, D. M.; Bergman, R. G. *J. Am. Chem. Soc.* **2000**, *122*, 954−955.
(4) Tellers, D. M.; Bergman, R. G. *Organometallics* **2001**, *20*, 4819−4832.
(5) Kitajima, N.; Tolman, W. B. *Prog. Inorg. Chem.* **1995**, *43*, 419−531.
(6) Koch, J. L.; Shapley, P. A. *Organometallics* **1997**, *16*, 4071−4076.
(7) Gutierrez-Puebla, E.; Monge, A.; Nicasio, M. C.; Perez, P. J.; Poveda, M. L.; Rey, L.; Ruiz, C.; Carmona, E. *Inorg. Chem.* **1998**, *37*, 4538−4546.
(8) Gutierrez-Puebla, E.; Monge, A.; Paneque, M.; Poveda, M. L.; Taboada, S.; Trujillo, M.; Carmona, E. *J. Am. Chem. Soc.* **1999**, *121*, 346−354.
(9) Barney, A. A.; Heyduk, A. F.; Nocera, D. G. *Chem. Commun.* **1999**, 2379−2380.
(10) Peters, J. C.; Feldman, J. D.; Tilley, T. D. *J. Am. Chem. Soc.* **1999**, *121*, 9871−9872.
(11) Schebler, P. J.; Riordan, C. G.; Guzei, I. A.; Rheingold, A. L. *Inorg. Chem.* **1998**, *37*, 4754−4755.

10.1021/om0205086 CCC: $22.00
Publication on Web 08/31/2002

Scheme 1

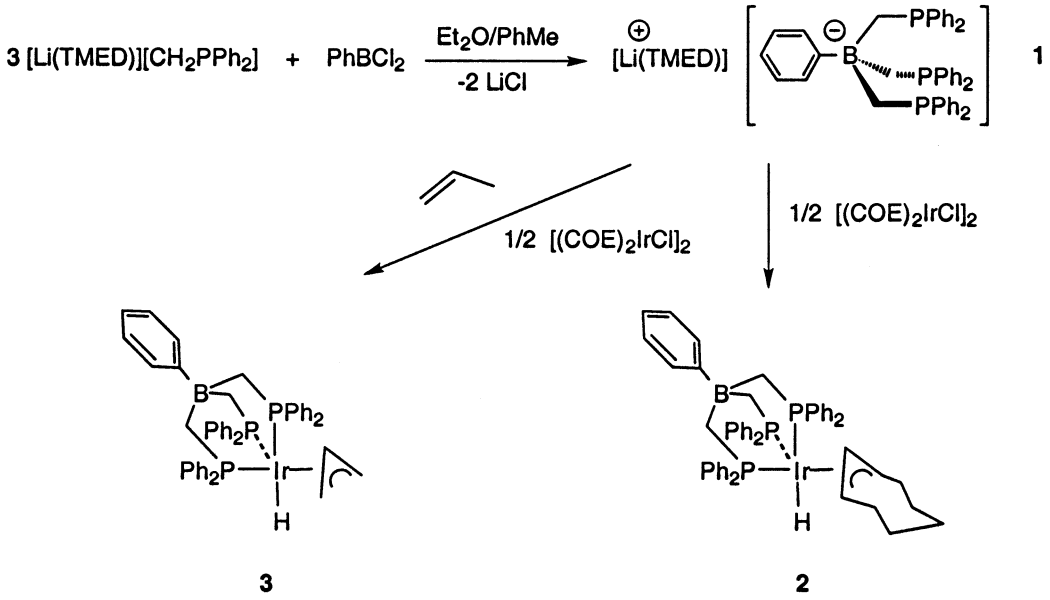

coordinates with three σ-donor atoms, as do Tp ligands. In a previous communication, a zwitterionic iridium complex featuring this ligand was shown to display a previously unknown reaction type in the extrusion of dimesitylsilylene from dimesitylsilane to give [$PhBP_3$]-$(H)_2Ir{=}SiMes_2$ (Mes = 2,4,6-trimethylphenyl).[10] This contribution describes the synthesis and reactivity of several new iridium complexes featuring this ligand. A comparison of the reactivity and properties of [$PhBP_3$]-Ir to those of analogous Cp*Ir and Tp^{Me_2}Ir fragments indicates that the [$PhBP_3$] ligand is strongly electron-donating toward iridium and is quite sterically demanding. Many studies have focused on the ability of complexes derived from Cp*Ir or Tp^{Me_2}Ir to activate C−H bonds.[12−20] As described here, C−H activations also occur readily in [$PhBP_3$]Ir complexes.

Results

Preparation of [$PhBP_3$]Ir Allyl Complexes. [Li-(TMED)][$PhBP_3$] (**1**; TMED = *N*,*N*,*N*′,*N*′-tetramethylethylenediamine) was readily prepared via the low-temperature addition of dichlorophenylborane to [Li-(TMED)][CH_2PPh_2] (3 equiv) in 72% yield as a colorless, crystalline solid (Scheme 1). The $^{31}P\{^1H\}$ NMR spectrum of **1** contains a single resonance at δ −12.4 for the equivalent phosphines, and ^1H NMR spectroscopy reveals that 1 equiv of TMED is retained in the product. The ^{11}B NMR shift for **1** (δ −14.0), as well as various iridium complexes prepared herein, is consistent with a four-coordinate borate of the type BR_4^-.[21]

Phosphine **1** undergoes salt metathesis with [$(COE)_2$-$IrCl]_2$ (COE = cyclooctene) to give zwitterionic [$PhBP_3$]-Ir(H)(η^3-C_8H_{13}) (**2**) via C−H activation of a COE ligand. Isolation of pure, colorless **2** from the greenish brown product mixture was difficult, due to the similar solubilities of the desired product and impurities. However, analytically pure **2** was obtained in 65−87% yield via multiple crystallizations from toluene. The $^{31}P\{^1H\}$ NMR spectrum of **2** contains a doublet (δ −7.77, $^2J_{PP}$ = 22 Hz) and a triplet (δ −13.37, $^2J_{PP}$ = 22 Hz) in a 2:1 ratio, consistent with a mirror plane of symmetry that bisects the [$PhBP_3$] ligand. Diagnostic features of the ^1H NMR spectrum include the allyl methine resonances (multiplets at δ 4.90 and 3.57) and an iridium hydride resonance (δ −12.55), which appears as a doublet of triplets due to large trans-phosphine coupling ($^2J_{HP(trans)}$ = 150 Hz) and significantly weaker coupling to the cis-phosphines ($^2J_{HP(cis)}$ = 14 Hz). These NMR data are consistent with the structure for **2** shown in Scheme 1. This transformation is analogous to that used to prepare TpIr(H)(COE)(η^1-C_8H_{13}) and TpIr(H)(η^3-C_8H_{13}) from KTp and [$(COE)_2IrCl]_2$.[22−24]

The allyl hydride complex [$PhBP_3$]Ir(H)(η^3-C_3H_5) (**3**) was obtained by addition of **1** to a THF solution of [$(COE)_2IrCl]_2$ that had been saturated with propene. No dark impurities were observed, unlike in the preparation of **2**; the color of the solution remained yellow throughout the reaction time of 24 h. Compound **3** was therefore easier to isolate and purify, and it was obtained in 72% yield after crystallization from THF. The $^{31}P\{^1H\}$ and ^1H NMR spectra of **3** are similar to

(12) For examples, see refs 4 and 13−20.
(13) Slugovc, C.; Padilla-Martinez, I.; Sirol, S.; Carmona, E. *Coord. Chem. Rev.* **2001**, *213*, 129−157.
(14) Slugovc, C.; Mereiter, K.; Trofimenko, S.; Carmona, E. *Angew. Chem., Int. Ed.* **2000**, *39*, 2158−2160.
(15) Gutierrez-Puebla, E.; Monge, A.; Nicasio, M. C.; Perez, P. J.; Poveda, M. L.; Carmona, E. *Chem. Eur. J.* **1998**, *4*, 2225−2236.
(16) Ghosh, C. K.; Hoyano, J. K.; Krentz, R.; Graham, W. A. G. *J. Am. Chem. Soc.* **1989**, *111*, 5480−5481.
(17) Rest, A. J.; Whitwell, I.; Graham, W. A. G.; Hoyano, J. K.; McMaster, A. D. *J. Chem. Soc., Dalton Trans.* **1987**, 1181−1190.
(18) Asbury, J. B.; Hang, K.; Yeston, J. S.; Cordaro, J. G.; Bergman, R. G.; Lian, T. Q. *J. Am. Chem. Soc.* **2000**, *122*, 12870−12871.
(19) Janowicz, A. H.; Bergman, R. G. *J. Am. Chem. Soc.* **1983**, *105*, 3929−3939.
(20) Tellers, D. M.; Yung, C. M.; Arndtsen, B. A.; Adamson, D. R.; Bergman, R. G. *J. Am. Chem. Soc.* **2002**, *124*, 1400−1410.
(21) Kidd, R. G. *NMR of Newly Accessible Nuclei*; Academic Press: New York, 1983; Vol. 2.
(22) Fernandez, M. J.; Rodriguez, M. J.; Oro, L. A.; Lahoz, F. J. *J. Chem. Soc., Dalton Trans.* **1989**, 2073−2076.
(23) Alvarado, Y.; Boutry, O.; Gutierrez, E.; Monge, A.; Nicasio, M. C.; Poveda, M. L.; Perez, P. J.; Ruiz, C.; Bianchini, C.; Carmona, E. *Chem., Eur. J.* **1997**, *3*, 860−873.
(24) Tanke, R. S.; Crabtree, R. H. *Inorg. Chem.* **1989**, *28*, 3444−3447.

Table 1. Crystallographic Data for Compounds 2−4 and 8

	2·THF	**3**·C_6H_6	**4**·CH_2Cl_2·C_5H_{12}	**8**·C_6H_6
empirical formula	$C_{57}H_{62}BP_3IrO$	$C_{54}H_{53}BP_3Ir$	$C_{54}H_{64}BP_4IrCl_2$	$C_{51}H_{49}BP_3Ir$
fw	1059.07	997.99	1110.98	957.93
cryst color, habit	yellow, plate	colorless, prism	colorless, block	orange, block
cryst size (mm)	0.18 × 0.16 × 0.02	0.32 × 0.30 × 0.15	0.22 × 0.14 × 0.13	0.27 × 0.05 × 0.02
cryst syst	triclinic	monoclinic	monoclinic	triclinic
space group	$P\bar{1}$ (No. 2)	$P2_1/n$ (No. 14)	$P2_1/n$ (No. 14)	$P\bar{1}$ (No. 2)
a (Å)	12.2337(7)	11.2342(2)	11.5654(2)	12.446(2)
b (Å)	13.2280(8)	17.0483(3)	22.8776(2)	13.005(2)
c (Å)	16.7505(10)	23.6861(5)	18.5238(2)	14.348(2)
α (deg)	92.164(1)	90	90	91.562(3)
β (deg)	108.453(1)	101.833(1)	98.72(1)	100.118(3)
γ (deg)	111.029(1)	90	90	113.984(3)
V (Å^3)	2364.7(2)	4440.1(1)	4844.5(1)	2081.4(5)
orientation rflns: no., 2θ range (deg)	4471, 3.0−46.0	8192, 3.0−46.0	8192, 3.0−46.0	992, 3.0−46.0
Z	2	4	4	4
D_{calcd} (g/cm^3)	1.487	1.394	1.405	1.468
F_{000}	1078.00	1872.00	2056.00	924.00
μ(Mo Kα) (cm^{-1})	29.73	31.55	30.36	33.64
diffractometer	SMART			
radiation	Mo Kα (λ = 0.710 69 Å), graphite monochromated			
temp (K)	155(1)	154(1)	150(1)	147(1)
scan type	ω (0.3° per frame)			
scan rate (s/frame)	10.0			
data collected, $2\theta_{max}$ (deg)	51.9	51.3	49.4	51.3
no. of rflns measd				
total	13 046	22 162	24 354	10 644
unique	7957	9110	8219	6717
R_{int}	0.049	0.048	0.067	0.037
transmissn factors				
T_{max}	0.93	0.69	0.65	0.95
T_{min}	0.57	0.54	0.34	0.61
structure soln	direct methods (SIR92)			
no. of obsd data ($I > 3\sigma(I)$)	5074	4968	4898	2102
no. of params refined	259	527	543	278
rfln/param ratio	19.59	9.43	9.02	7.56
final residuals: R; R_w; R_{all}[a]	0.045; 0.043; 0.087	0.028; 0.032; 0.063	0.035; 0.037; 0.069	0.050; 0.050; 0.106
goodness-of-fit indicator[b]	1.13	1.19	0.99	1.02
max shift/error final cycle	0.01	0.00	0.04	0.00
max, min peaks, final diff map (e/Å^3)	1.20, −0.91	1.97, −1.11	1.34, −1.85	1.81, −1.24

[a] $R = \sum||F_o| - |F_c||/\sum|F_o|$; $R_w = [\sum w(|F_o| - |F_c|)^2/\sum wF_o^2]^{1/2}$. [b] Goodness of fit = $[\sum w(|F_o| - |F_c|)^2/(N_{observns} - N_{params})]^{1/2}$.

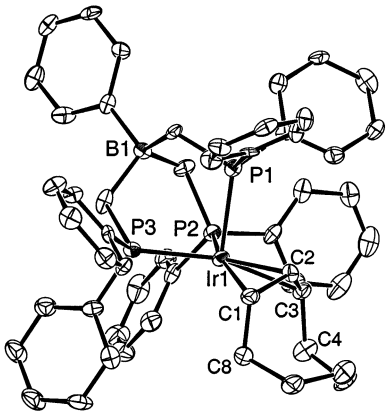

Figure 1. ORTEP diagram of [$PhBP_3$]Ir(η^3-C_8H_{13})H (**2**).

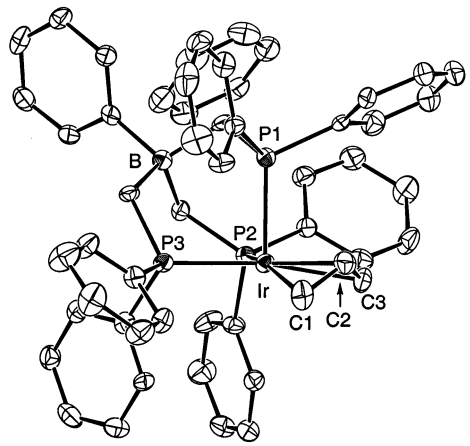

Figure 2. ORTEP diagram of [$PhBP_3$]Ir(η^3-C_3H_5)H (**3**).

those of **2** and are consistent with its characterization as an η^3-allyl hydride complex.

The solid-state structures of **2** and **3** (Figures 1 and 2, respectively) were determined by single-crystal X-ray diffraction; selected bond distances and angles are listed in Tables 2 and 3. The expected facial coordination of the tripodal phosphine ligand in both cases is reflected in P−Ir−P angles of approximately 90° (88−90° for **2**; 87−91° for **3**). The C−Ir bond distances for the η^3-allyl ligands range from 2.18 to 2.30 Å for **2** and from 2.19 to 2.26 Å for **3**. These distances are similar to those found in other Ir(III) allyl complexes, which are on average 2.24 Å.[23,25−33] The position of the hydride ligand was not determined for either **2** or **3**; however, its approximate location is indicated by the open coordination site trans to P(1). The greater trans influence of the hydride relative to the η^3-allyl ligand is reflected in

Table 2. Selected Bond Distances (Å) and Angles (deg) for 2

(a) Bond Distances			
Ir1−P1	2.409(2)	Ir1−C2	2.176(8)
Ir1−P2	2.304(2)	Ir1−C3	2.261(9)
Ir1−P3	2.311(2)	C1−C2	1.43(1)
Ir1−C1	2.302(9)	C2−C3	1.43(1)
(b) Bond Angles			
P1−Ir1−P2	87.96(8)	C1−C2−C3	120.9(8)
P1−Ir1−P3	90.31(8)	C2−C1−C8	123.0(8)
P2−Ir1−P3	90.11(8)	C2−C3−C4	124.0(7)

Table 3. Selected Bond Distances (Å) and Angles (deg) for 3

(a) Bond Distances			
Ir−P1	2.388(2)	Ir−C2	2.186(6)
Ir−P2	2.320(1)	Ir−C3	2.234(6)
Ir−P3	2.307(2)	C1−C2	1.405(9)
Ir−C1	2.255(6)	C2−C3	1.402(9)
(b) Bond Angles			
P1−Ir−P2	91.05(5)	P2−Ir−P3	87.47(6)
P1−Ir−P3	89.69(6)	C1−C2−C3	121.9(6)

the elongated Ir−P(1) distance of 2.408(2) Å, which may be compared to the Ir−P(2) and Ir−P(3) distances of 2.304(2) and 2.311(2) Å, respectively, for **2** (2.388(2) vs 2.320(1) and 2.307(2) Å for **3**).

Reactions of [PhBP$_3$]Ir Allyl Complexes with Phosphines. Reaction of **2** with PMe_3 (1.4 equiv, room temperature, 3 h) in benzene-d_6 resulted in intramolecular metalation to give **4** (eq 1) with the concomitant formation of COE. $^{31}P\{^1H\}$ NMR spectroscopy indicates

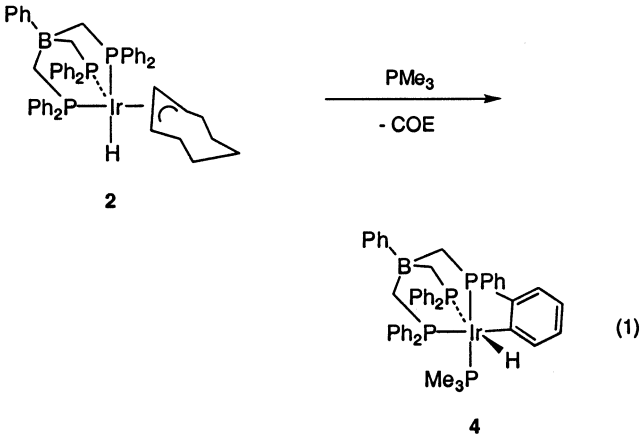

2 **4** (1)

quantitative formation of a product with four inequivalent phosphorus atoms. Two of these P atoms are trans to one another (δ −59.22, −72.67, $^2J_{PP(trans)} = 282$ Hz), and two are cis to three other phosphines (δ −1.87, −17.55, $^2J_{PP(cis)} = 18$ Hz). Also, 1 equiv of free COE and an iridium hydride resonance (δ −9.32, $^2J_{HP(trans)} = 121$ Hz) are observed in the ^1H NMR spectrum. These data suggest a product derived from intramolecular C−H activation of one of the P−Ph groups to give the ortho-metalated complex {PhB[$(CH_2PPh_2)_2(CH_2PPhC_6H_4)$]}Ir(H)($PMe_3$) (**4**). Formation of the four-membered ring in complex **4** may be irreversible, as prolonged thermolysis of **4** in benzene-d_6 (85 °C, 1 week) failed to produce any new products resulting from C−D activation (by $^{31}P\{^1H\}$ and ^1H NMR spectroscopy). Upon scale-up and

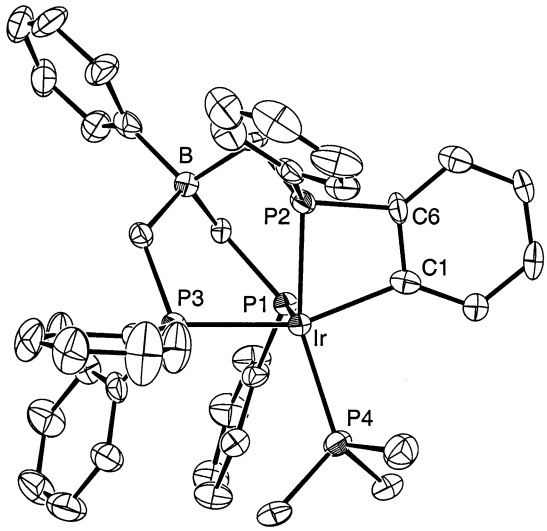

Figure 3. ORTEP diagram of {PhB[$(CH_2PPh_2)_2(CH_2PPhC_6H_4)$]}Ir(H)($PMe_3$) (**4**), in which one of the phenyl groups on P1 has been omitted for clarity.

Table 4. Selected Bond Distances (Å) and Angles (deg) for 4

(a) Bond Distances			
Ir−P1	2.377(2)	Ir−P4	2.325(2)
Ir−P2	2.320(2)	Ir−C1	2.116(7)
Ir−P3	2.377(2)	C1−C6	1.40(1)
(b) Bond Angles			
P1−Ir−P2	91.22(6)	P3−Ir−P4	107.39(7)
P1−Ir−P3	88.41(7)	C1−Ir−P1	90.2(2)
P1−Ir−P4	105.84(7)	C1−Ir−P2	67.6(2)
P2−Ir−P3	90.51(6)	C1−Ir−P3	158.1(2)
P2−Ir−P4	155.28(7)	C1−Ir−P4	94.0(2)

crystallization from CH_2Cl_2, pure **4**·$2CH_2Cl_2$ was isolated in 92% yield.

The structure of **4** was confirmed by X-ray crystallography; an ORTEP diagram is depicted in Figure 3, and selected bond distances and angles are given in Table 4. The facially coordinating [PhBP$_3$] ligand gives rise to P−Ir−P angles ranging from 88 to 91°, but the remaining iridium−ligand bonds reflect substantial distortions from ideal octahedral geometry. The four-membered $IrPC_2$ ring confines the geometry of this complex, resulting in C(1)−Ir−P angles of 67.6(2), 90.2(2), 94.0(2), and 158.1(2)°. Likewise, the PMe_3 ligand is tilted away from the two bulky phosphine ligands (P(4)−Ir−P(1) and P(4)−Ir−P(3) angles of 105.84(7) and 107.39(7)°, respectively), giving rise to a P(4)−Ir−P(2) angle of 155.28(7)°. The hydride ligand was not located by X-ray diffraction, but its position is assumed to be in the otherwise open coordination site trans to P(1). Overall, the structure of **4** is similar to that of the related complex *cis*-$(Ph_3P)_2(Ph_2PC_6H_4)$Ir(H)(Br).[34]

A dissimilar reaction occurred upon thermolysis of **2** in the presence of $PMePh_2$ (80 °C, benzene, 24 h). In this case the allyl complex was observed to undergo β-H elimination to give 1,3-cyclooctadiene (1,3-COD, by GC/MS and ^1H NMR spectroscopy), and the coordination of $PMePh_2$ to iridium gave [PhBP$_3$]Ir($PMePh_2$)H_2 (**5**; eq 2) in 46% isolated yield. Complex **5** has C_s symmetry,

(25) Hsu, R. H.; Chen, J. T.; Lee, G. H.; Wang, Y. *Organometallics* **1997**, *16*, 1159−1166.
(26) Schnabel, R. C.; Roddick, D. M. *Organometallics* **1996**, *15*, 3550−3555.
(27) Wakefield, J. B.; Stryker, J. M. *Organometallics* **1990**, *9*, 2428−2430.
(28) Merola, J. S. *Organometallics* **1989**, *8*, 2975−2977.
(29) McGhee, W. D.; Hollander, F. J.; Bergman, R. G. *J. Am. Chem. Soc.* **1988**, *110*, 8428−8443.
(30) McGhee, W. D.; Bergman, R. G. *J. Am. Chem. Soc.* **1986**, *108*, 5621−5622.
(31) Tulip, T. H.; Ibers, J. A. *J. Am. Chem. Soc.* **1979**, *101*, 4201−4211.
(32) Schoonover, M. W.; Baker, E. C.; Eisenberg, R. *J. Am. Chem. Soc.* **1979**, *101*, 1880−1882.
(33) Kaduk, J. A.; Poulos, A. T.; Ibers, J. A. *J. Organomet. Chem.* **1977**, *127*, 245−260.
(34) Vondeuten, K.; Dahlenburg, L. *Cryst. Struct. Commun.* **1980**, *9*, 421−427.

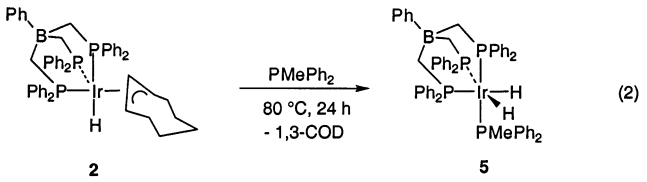

(2)

with a mirror plane that contains the iridium center, the phosphorus donor of the $PMePh_2$ ligand, and one of the phosphine donors of the [$PhBP_3$] ligand. The equivalent hydride ligands give rise to a ^1H NMR resonance at δ −11.04 (dm, $^2J_{HP(trans)} = 107$ Hz). The $^{31}P\{^1H\}$ NMR spectrum of **5** displays an A_2MX pattern; two of the [$PhBP_3$] phosphorus atoms are equivalent and trans to hydride ligands (δ −10.42, t, $^2J_{PP(cis)} = 21$ Hz), and the third [$PhBP_3$] phosphorus atom and $PMePh_2$ are trans to one another (δ −0.98 and −16.84, respectively; $^2J_{PP(trans)} = 285$ Hz).

Reactions of [$PhBP_3$]Ir($PMePh_2$)H_2 (5). Photolysis of **5** (benzene-d_6, 13 h) resulted in elimination of H_2, and intramolecular C−H activation occurred exclusively (no C−D activation of benzene-d_6 by NMR spectroscopy). A mixture of two products was observed, and on the basis of spectroscopic properites we propose that these are derived from ortho metalation of the [$PhBP_3$] and $PMePh_2$ phenyl groups (**A** and **B** in eq 3). Like metalation product **4**, **A** and **B** exhibit A_2MX patterns in their $^{31}P\{^1H\}$ NMR spectra. The ratio of **A** to **B** is 2:5, indicating that C−H activation of the eight P-phenyl substituents is nearly statistical (2:6).

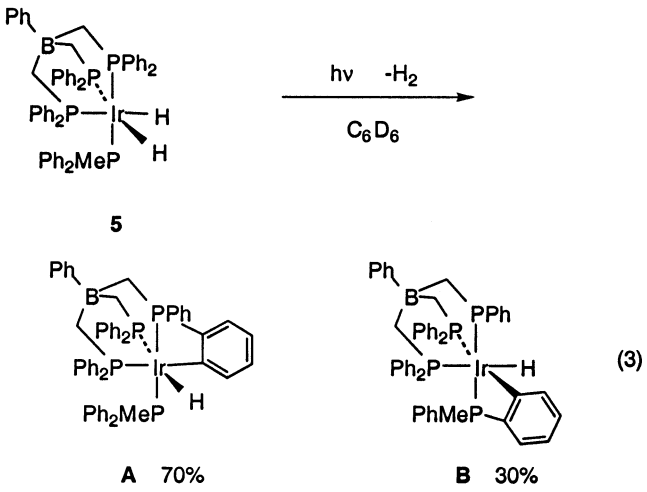

(3)

A variety of Tp′Ir(PR_3)H_2 and Cp′Ir(PR_3)H_2 complexes (where Tp′ is Tp or Tp^{Me_2} and Cp′ is Cp or Cp*) are known to undergo protonation to give cationic hydrides. While Cp′Ir(PR_3)H_3^+ complexes are classical hydrides, as determined by neutron diffraction studies,[35−37] Tp′Ir(PR_3)(H_2)$(H)^+$ derivatives adopt nonclassical structures, as determined by T_1(min) ^1H NMR data.[38]

Protonation of **5** with [$H(OEt_2)_2$]{B[3,5-$C_6H_3(CF_3)_2]_4$}[39] gave the new cationic hydride {[$PhBP_3$]Ir($PMePh_2$)H_3}{B[3,5-$C_6H_3(CF_3)_2]_4$} (**6**), which exhibits a shift of δ −11.21 for the hydride ligands (dm, $^2J_{HP} = 112$ Hz) by ^1H NMR spectroscopy. The T_1(min) value for this resonance was determined to be 281 ± 5 ms (−18 °C, CD_2Cl_2, 500 MHz), while that of the IrH resonance for **5** is 274 ± 5 ms (−28 °C, CD_2Cl_2, 500 MHz). Both T_1(min) values are well within the range expected for classical hydride complexes.[40,41]

Preparation of [$PhBP_3$]Ir$(CO)_2$. The preparation of carbonyl complexes of the [$PhBP_3$]Ir fragment was of interest, since the ν(CO) stretching frequencies of such species should provide information regarding the electronic properties of the [$PhBP_3$] ligand. Complexes **2** and **3** reacted with carbon monoxide (1 atm, 80 °C, benzene) over several days to give cyclooctene and propene, respectively, and an iridium-containing product (**7**) that exhibits a single $^{31}P\{^1H\}$ NMR resonance at δ −10.6. When ^{13}CO was employed in the synthesis of **7**, this ^{31}P NMR resonance appeared as a triplet ($^2J_{PC}$ = 24 Hz), indicating the coordination of two carbonyl ligands to give the 18-electron Ir(I) species [$PhBP_3$]Ir$(CO)_2$, as shown in eq 4. The IR spectrum of **7** in hexanes contains CO stretching frequencies of 2024 and 1940 cm^{-1}.

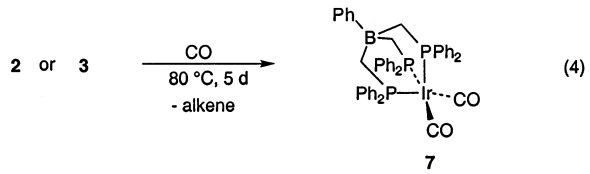

(4)

Reactions of the Allyl Complexes with H_2. Heating a benzene solution of **2** under 1 atm of H_2 (80 °C, 19 h) produced COE (by ^1H NMR spectroscopy) and an orange crystalline compound (**8**; Scheme 2). The hydrogenation of **3** (benzene-d_6, 80 °C, 48 h) also yielded polyhydride **8**, as well as propane (by ^1H NMR spectroscopy). Complex **8** is insoluble in a wide range of solvents (benzene, THF, CH_2Cl_2, C_6H_5F, DMSO, DMF, dioxane) and was therefore characterized by IR spectroscopy, X-ray crystallography, and elemental analysis (but not NMR spectroscopy).

Scheme 2

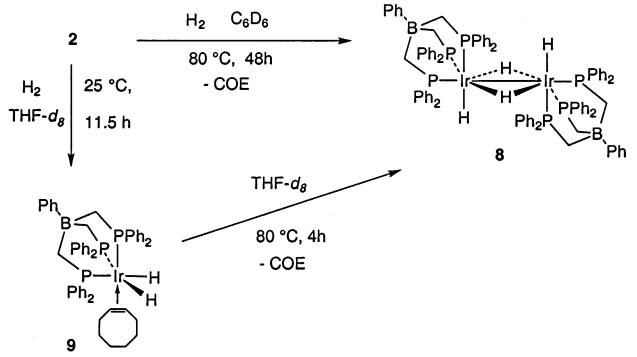

An X-ray diffraction study revealed a dimeric structure for **8** (Figure 4; selected bond distances and angles

(35) Zilm, K. W.; Heinekey, D. M.; Millar, J. M.; Payne, N. G.; Neshyba, S. P.; Duchamp, J. C.; Szczyrba, J. *J. Am. Chem. Soc.* **1990**, *112*, 920−929.

(36) Heinekey, D. M.; Millar, J. M.; Koetzle, T. F.; Payne, N. G.; Zilm, K. W. *J. Am. Chem. Soc.* **1990**, *112*, 909−919.

(37) Heinekey, D. M.; Hinkle, A. S.; Close, J. D. *J. Am. Chem. Soc.* **1996**, *118*, 5353−5361.

(38) Oldham, W. J.; Hinkle, A. S.; Heinekey, D. M. *J. Am. Chem. Soc.* **1997**, *119*, 11028−11036.

(39) Brookhart, M.; Grant, B.; Volpe, A. F. *Organometallics* **1992**, *11*, 3920−3922.

(40) Crabtree, R. H.; Lavin, M.; Bonneviot, L. *J. Am. Chem. Soc.* **1986**, *108*, 4032−4037.

(41) Crabtree, R. H.; Hamilton, D. G. *J. Am. Chem. Soc.* **1986**, *108*, 3124−3125.

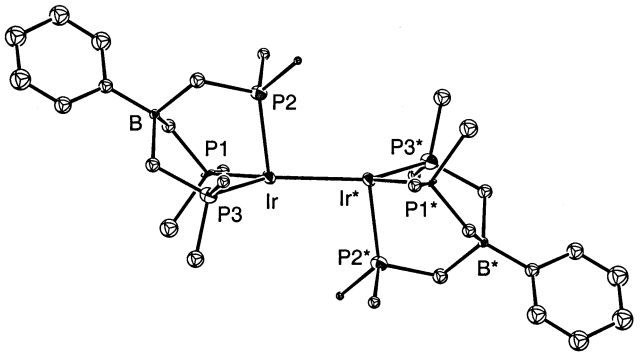

Figure 4. ORTEP diagram of $\{[PhBP_3]Ir(H)(\mu\text{-}H)\}_2$ (**8**).

Table 5. CO Stretching Frequencies for $LIr(CO)_2$ Complexes in Hexanes

complex	ν(CO), cm^{-1}
$Tp^{Me_2}Ir(CO)_2$	2039, 1960
$Cp^*Ir(CO)_2$	2020, 1953
$[PhBP_3]Ir(CO)_2$	2024, 1940

Table 6. Selected Bond Distances (Å) and Angles (deg) for 8

	(a) Bond Distances		
Ir−P1	2.298(6)	Ir−P3	2.309(6)
Ir−P2	2.415(6	Ir−Ir*	2.796(2)
	(b) Bond Angles		
P1−Ir−P2	89.5(2)	P1−Ir−Ir*	137.3(1)
P1−Ir−P3	84.1(2)	P2−Ir−Ir*	98.2(1)
P2−Ir−P3	90.5(2)	P3−Ir−Ir*	137.3(2)

are given in Table 6), in which the halves of the molecule are related by a crystallographic inversion center. Very few diiridium complexes containing only hydrides as bridging ligands have been structurally characterized. The four such structures in the Cambridge Structural Database (CSD) have Ir−Ir distances ranging from 2.46 to 2.98 Å and include $[(Cp^*Ir)_2(\mu_2\text{-}H)_3][ClO_4]$,[42] $\{[Cp^*(PMe_3)(H)Ir]_2(\mu_2\text{-}H)\}_2[PF_6]$,[43] $\{[(Ph_2PCH_2CH_2PPh_2)Ir(H)]_2(\mu_2\text{-}H)_3\}[BF_4]$,[44] and $[\{(C_2F_6)_2PCH_2CH_2P(C_2F_6)_2\}(H)_2Ir(\mu_2\text{-}H)]_2$.[45] In **8**, the Ir−Ir distance of 2.797(2) Å is somewhat longer than the average distance of the previously reported structures (2.62 Å). The tridentate phosphine ligand is unsymmetrically coordinated with respect to the Ir−Ir bond axis, resulting in P−Ir−Ir angles of 137.3(1), 98.2(1), and 137.3(1)°. Although the hydride ligands were not located in the structure refinement, the positions of the terminal hydrides are indicated by the open coordination sites arising from the tilt of the triphosphine ligand (see Figure 4).

The X-ray structure suggests a di- or trihydride dimer of the type $\{[PhBP_3]Ir(H)_x(\mu\text{-}H)\}_2$, where $x = 1, 2$. For the case where $x = 2$, $\{[PhBP_3]Ir(H)_2(\mu\text{-}H)\}_2$ has two terminal hydrides and an iridium−iridium single bond and contains (formally) Ir(IV) centers. A similar complex, $[Cp^*Ir(H)_2(\mu\text{-}H)]_2$, has been reported by Bergman and co-workers.[46] A rhodium compound related to the latter hydride complex where $x = 1$, $[(triphos)RhH(\mu\text{-}H)]_2[BPh_4]_2$ (triphos = $MeC(CH_2PPh_2)_3$), has been prepared by Bianchini and co-workers.[47]

The IR spectrum (KBr) of **8** features an absorption at 2114 cm^{-1}, which we attribute to the terminal Ir−H stretch. Although the bridging Ir−H stretch could not be identified with certainty, a peak observed at 1088 cm^{-1} is consistent with literature values for related species.[46,48,49] To confirm these assignments, we attempted to label the hydride ligands by carrying out the reaction of **3** with D_2 in benzene-d_6 (73 °C, 15 h). This led to formation of an orange solid and a ca. 1:1 mixture of COE and COE-d_{14} (by ^1H and $^2H\{^1H\}$ NMR spectroscopy and GC/MS). An IR spectrum of the solid suggests that the hydride positions of **8** are only partially deuterated. Although the peak assigned to the terminal Ir−H stretch (2114 cm^{-1}) of **8** is present, it has a reduced intensity relative to the other peaks in the spectrum. Furthermore, a new peak at 1514 cm^{-1} is present, which may be attributed to a terminal Ir−D stretch. Scrambling of the ortho hydrogens of the PPh_2 substituent with the iridium hydride positions could account for the formation of a mixture of **8** and **8**-d_x. We have observed a related scrambling process in which deuterium is incorporated into the ortho hydrogen positions of the $[PhBP_3]$ ligand in reactions of **2** with Mes_2SiD_2[50] and have characterized an ortho-metalated product of this ligand (**4**; vide supra).

To determine the exact formula for dimer **8**, we attempted to independently generate the two possible structures, $\{[PhBP_3]Ir(H)_x(\mu\text{-}H)\}_2$, where $x = 1, 2$. Toward this end we discovered that $[PhBP_3]Ir(COE)H_2$ (**9**) could be prepared by the hydrogenation of **3** in THF (rather than in benzene). This reaction also produces the insoluble dimer **8** as a side product (by IR spectroscopy). The yield of **9** (59%) was optimized by performing the hydrogenation (1 atm, room temperature, 11.5 h) in the presence of excess COE. It was anticipated that isolated **9** could serve as a precursor to $\{[PhBP_3]Ir(H)(\mu\text{-}H)\}_2$, because it contains two hydride ligands and a potential leaving group (COE). Indeed, thermolysis of **9** (THF-d_8, 80 °C, 4 h) resulted in quantitative formation of **8** (by IR spectroscopy) and COE. Therefore, mass balance dictates that **8** must be the dihydride dimer $\{[PhBP_3]Ir(H)(\mu\text{-}H)\}_2$. Its formation presumably comes about via dissociation of COE from **9** to give $[PhBP_3]Ir(H)_2$, which then irreversibly dimerizes (Scheme 2).

Two additional decomposition pathways for **9** have been observed. Thermolysis of **9** in benzene-d_6 (85 °C, 2 h) instead of THF-d_8 gave **8** and COE-d_{14} (presumably via activation of the solvent; see Discussion). Also, photolysis of **9** (benzene-d_6, 5 h) gave **8** and COE (undeuterated) and a small amount of H_2 and allyl **2** (<10%, by NMR spectroscopy).

Preparation of $[PhBP_3]IrX_2$ (X = I, Cl) Complexes. Attempts to obtain simple dihalide complexes of the type $[PhBP_3]IrX_2$ were based on the assumption that such species could serve as useful starting materials for elaboration of the chemistry of the $[PhBP_3]Ir$

(42) Stevens, R. C.; McLean, M. R.; Wen, T.; Carpenter, J. D.; Bau, R.; Koetzle, T. F. *Inorg. Chim. Acta* **1989**, *161*, 223−231.
(43) Burns, C. J.; Rutherford, N. M.; Berg, D. J. *Acta Crystallogr., Sect. C: Cryst. Struct. Commun.* **1987**, *43*, 229−231.
(44) Wang, H. H.; Pignolet, L. H. *Inorg. Chem.* **1980**, *19*, 1470−1480.
(45) Schnabel, R. C.; Carroll, P. S.; Roddick, D. M. *Organometallics* **1996**, *15*, 655−662.
(46) Gilbert, T. M.; Hollander, F. J.; Bergman, R. G. *J. Am. Chem. Soc.* **1985**, *107*, 3508−3516.
(47) Bianchini, C.; Meli, A.; Laschi, F.; Ramirez, J. A.; Zanello, P.; Vacca, A. *Inorg. Chem.* **1988**, *27*, 4429−4435.
(48) Gill, D. S.; Maitlis, P. M. *J. Organomet. Chem.* **1975**, *87*, 359−364.
(49) White, C.; Oliver, A. J.; Maitlis, P. M. *J. Chem. Soc., Dalton Trans.* **1973**, 1901−1907.
(50) Feldman, J. D.; Peters, J. C.; Tilley, T. D. *Organometallics*, in press.

fragment. A blood red solution of $[PhBP_3]IrI_2$ (**10**) was formed upon addition of a benzene solution of I_2 to a benzene/acetonitrile (3:2) solution of **2** (eq 5). The

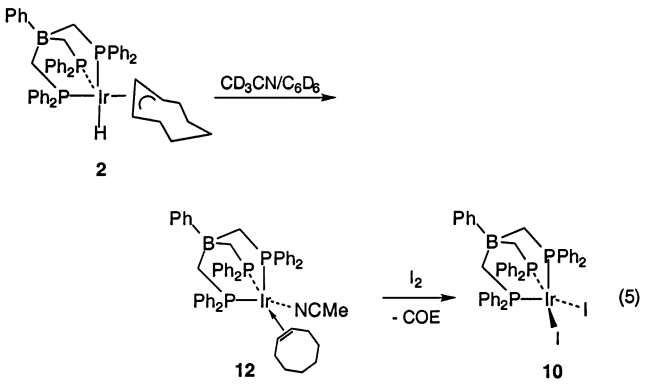

diiodide **10** was isolated in 94% yield as maroon-purple crystals after solvent removal and washing with pentane. The dichloride **11** was prepared by heating a benzene/CCl_4 (1:1) solution of **2** (or **3**) at 65−70 °C for 1 week, over which time a significant amount of orange **11** crystallized from solution (eq 6). The remaining

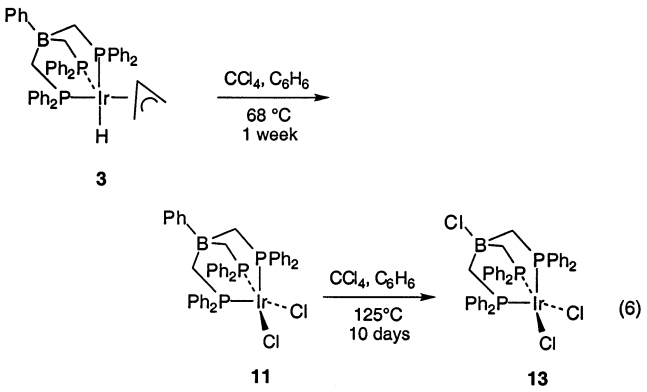

product was isolated in 97% yield upon solvent removal and washing with pentane.

Clean formation of **10** from **2** and I_2 was not observed unless a mixture of benzene and acetonitrile (3:2) was used as the solvent. NMR spectroscopy suggests that the presence of excess acetonitrile leads to formation of $[PhBP_3]Ir(\eta^2\text{-COE})(NCMe)$ (**12**). The ^1H NMR spectrum of **12** features an iridium-coordinated alkene resonance at δ 2.61 (vs δ 5.65 for free COE), and the $^{31}P\{^1H\}$ NMR spectrum reveals a complex with C_s symmetry consisting of a triplet and a doublet in a 2:1 ratio (δ −8.36, −15.69, $J_{PP(cis)} = 23$ Hz). The acetonitrile-promoted C−H reductive elimination to form this cyclooctene complex is reversible, and removal of the solvent under reduced pressure resulted in complete conversion of the equilibrium mixture to **2**.

When the reaction of **2** with benzene/CCl_4 (1:1) was carried out at temperatures greater than 90 °C, a byproduct containing a B−Cl bond was observed. This species, $[ClB(CH_2PPh_2)_3]IrCl_2$ (**13**; eq 6), was isolated as orange crystals in 24% yield upon thermolysis of **3** in benzene/CCl_4 (1:1) at 125 °C for 10 days.

Single-crystal X-ray diffraction studies of **10** and **13** show that these species are monomeric in the solid state. ORTEP diagrams of **10** and **13** are displayed in Figures 5 and 6, respectively, and selected bond distances and

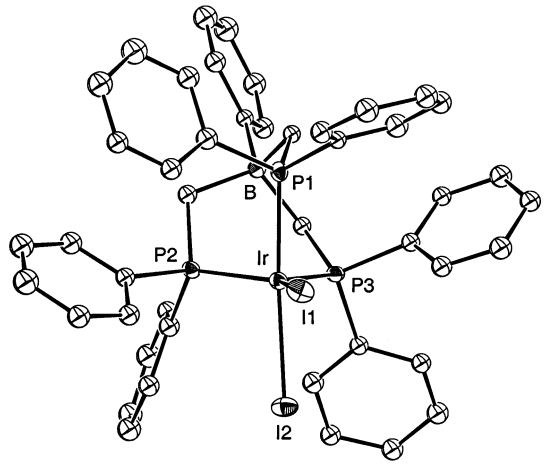

Figure 5. ORTEP diagram of $[PhBP_3]IrI_2$ (**10**).

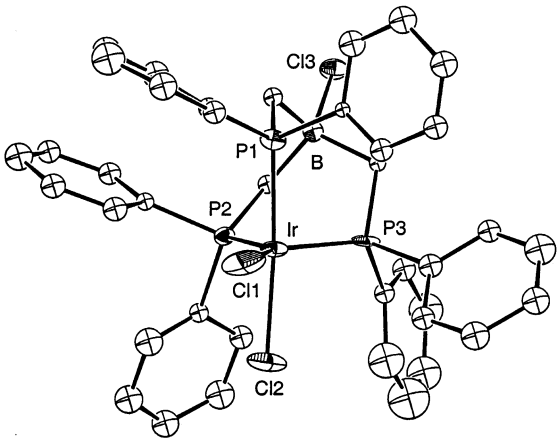

Figure 6. ORTEP diagram of $[ClB(CH_2PPh_2)_3]IrCl_2$ (**13**).

angles for **10** and **13** are listed in Tables 8 and 9, respectively. Both complexes exhibit a pseudo-trigonal-bipyramidal geometry with one halide in the axial position (I(2)−Ir−P angles of 173.40(7), 98.34(7), and 91.99(7)° for **10** and Cl(2)−Ir−P angles of 171.8(3), 93.4(2), and 96.5(3)° for **13**) and the other halide in the basal plane (I(1)−Ir−P angles of 88.83(7), 134.74(7), and 137.20(7)° for **10** and Cl(1)−Ir−P angles of 88.2(2), 137.1(3), and 137.5(3)° for **13**). The P−Ir−P angles in both complexes are approximately 90°.

For **10**, **11**, and **13**, only a single ^{31}P NMR resonance is observed in toluene-d_8 over the temperature range of 23 to −94 °C (δ 4.34, 4.92, and 0.93, respectively). A dimeric structure of the type $\{[PhBP_3]Ir(X)(\mu\text{-}X)\}_2$ would give rise to two coupled resonances (AB_2 spin system), as would a monomeric trigonal-bipyramidal structure. This implies that these molecules are fluxional in solution.

Reactions of the Dihalides 10 and 11. Initial studies indicate that the dihalide complexes **10** and **11** are useful starting materials for metathesis reactions. Two equivalents of $LiBHEt_3$ (1 M in THF) reacted with **10** or **11** (in benzene-d_6) to give $[Li(THF)_n]\{[PhBP_3]Ir(H)_2X\}$, where X = I (**14a**), Cl (**14b**), as shown in Scheme 3. While formation of **14a** is quantitative (by ^1H NMR spectroscopy), the addition of 2 equiv of $LiBHEt_3$ to **11** gives a mixture of hydride complexes, including **14b** (ca. 70%) as well as the trihydride $[Li(THF)_n]\{[PhBP_3]IrH_3\}$ (**15**; ca. 20%). Complex **15** is formed exclusively with the addition of 3 equiv of $LiBHEt_3$ to **10** or **11**. In each

Table 7. Crystallographic Data for Compounds 10, 13, and 16

	10·$2C_7H_8$	**13**	**16**·C_6H_6
empirical formula	$C_{59}H_{57}BP_3IrI_2$	$C_{45}H_{41}BP_3IrCl_3$	$C_{60}H_{58}BIrP_3$
fw	1315.90	984.16	1074.30
cryst color, habit	purple-red, block	orange, block	red, block
cryst size (mm)	0.18 × 0.11 × 0.02	0.11 × 0.08 × 0.04	0.28 × 0.10 × 0.05
crystal syst	monoclinic	triclinic	triclinic
space group	$P2_1/c$ (No. 14)	$P\bar{1}$ (No. 2)	$P\bar{1}$ (No. 2)
a (Å)	12.5190(4)	9.866(2)	10.523(1)
b (Å)	33.126(1)	10.655(2)	10.665(1)
c (Å)	12.2897(5)	19.045(4)	20.764(2)
α (deg)	90	101.112(3)	95.787(1)
β (deg)	91.511(1)	98.820(3)	91.028(1)
γ (deg)	90	109.347(3)	110.780(1)
V (Å^3)	5094.7(5)	1801.7(6)	2170.2(6)
orientation rflns: no., 2θ range (deg)	4861, 3.0−46.0	2607, 3.0−46.0	3163, 3.0−45.0
Z	4	2	2
D_{calcd} (g/cm^3)	1.491	1.300	1.286
F_{000}	2200.00	944.00	800.00
μ(Mo Kα) (cm^{-1})	39.61	41.00	32.24
diffractometer	SMART		
radiation	Mo Kα (λ = 0.710 69 Å), graphite monochromated		
temp (K)	126(1)	129(1)	138(1)
scan type		ω (0.3° per frame)	
scan rate (s/frame)	10.0	20.0	20.0
data collected, $2\theta_{max}$ (deg)	49.4	49.6	46.5
no. of rflns measd			
total	22 703	9224	5048
unique	8539	5760	4557
R_{int}	0.077	0. 086	0.056
transmissn factors			
T_{max}	0.86	0.75	0.96
T_{min}	0.54	0.62	0.54
structure soln		direct methods (SIR92)	
no. of obsd data ($I > 3\sigma(I)$)	4372	2501	3706
no. of params refined	365	224	253
rfln/param ratio	11.98	11.17	14.65
final residuals: R; R_w; R_{all}[a]	0.037; 0.040; 0.092	0.070; 0.080; 0.130	0.050; 0.062; 0.062
goodness-of-fit indicator[b]	0.95	1.4	2.44
max shift/error final cycle	0.05	0.00	0.02
max, min peaks, final diff map (e/Å^3)	1.39, −1.70	3.07, −2.61	2.03, −3.28

[a] $R = \sum||F_o| - |F_c||/\sum|F_o|$; $R_w = [\sum w(|F_o| - |F_c|)^2/\sum wF_o2]^{1/2}$. [b] Goodness of fit = $[\sum w(|F_o| - |F_c|)^2/(N_{observns} - N_{params})]^{1/2}$.

Table 8. Selected Bond Distances (Å) and Angles (deg) for 10

	(a) Bond Distances		
Ir−P1	2.357(3)	Ir−I1	2.6697(8)
Ir−P2	2.280(3)	Ir−I2	2.7086(8)
Ir−P3	2.274(3)		
	(b) Bond Angles		
P1−Ir−P2	87.6(1)	I1−Ir−P2	134.74(7)
P1−Ir−P3	91.01(9)	I1−Ir−P3	137.20(7)
P2−Ir−P3	88.0(1)	I2−Ir−P1	173.40(7)
I1−Ir−I2	84.98(3)	I2−Ir−P2	98.34(7)
I1−Ir−P1	88.83(7)	I2−Ir−P3	91.99(7)

Table 9. Selected Bond Distances (Å) and Angles (deg) for 13

	(a) Bond Distances		
Ir−P1	2.337(7)	Ir−Cl1	2.331(7)
Ir−P2	2.277(7)	Ir−Cl2	2.369(7)
Ir−P3	2.255(8)	B−Cl3	1.93(3)
	(b) Bond Angles		
P1−Ir−P2	91.0(2)	Cl1−Ir−P2	137.1(3)
P1−Ir−P3	90.7(2)	Cl1−Ir−P3	137.5(3)
P2−Ir−P3	85.4(2)	Cl2−Ir−P1	171.8(3)
Cl1−Ir−Cl2	83.9(3)	Cl2−Ir−P2	93.4(2)
Cl1−Ir−P1	171.8(3)	Cl2−Ir−P3	96.5(3)

reaction, free BEt_3 was observed (by ^{11}B NMR spectroscopy). These ate complexes were characterized spectroscopically and by derivatization chemistry, since attempts to isolate **14** and **15** resulted in decomposition.

The monohalide dihydride complexes **14a** and **14b** have very similar spectroscopic properties. The $^{31}P\{^1H\}$ NMR spectrum of **14a** contains two resonances, a triplet (δ 7.9, $^2J_{PP}$ = 11 Hz) and a doublet (δ −17.7, $^2J_{PP}$ = 11 Hz), in a 1:2 ratio. The corresponding resonances for **14b** occur at δ 9.1 (t, $^2J_{PP}$ = 14 Hz) and δ −9.2, (d, $^2J_{PP}$ = 14 Hz). The ^1H NMR spectra of **14a** and **14b** feature hydride resonances at δ −12.10 (dm, $^2J_{HP(trans)}$ = 124 Hz) and δ −10.12 (dm, $^2J_{HP(trans)}$ = 125 Hz), respectively. The $^{31}P\{^1H\}$ NMR spectrum of complex **15** in benzene-d_6 consists of a singlet (δ 1.40), and in the ^1H NMR spectrum the IrH resonance is observed at δ −12.42 (dm, $^2J_{HP(trans)}$ = 96 Hz).

Consistent with the formulation of **14a** as $[Li(THF)_n]$-$\{[PhBP_3]IrH_2I\}$, it was observed to react with $PMePh_2$ (13 equiv, room temperature, 5.5 h) to give $[PhBP_3]Ir(PMePh_2)H_2$ (**5**; by NMR spectroscopy) via the substitution of I^- with the phosphine. Due to the lower stability and transient nature of **14b** relative to **14a**, we have been unable to observe its transformation to **5** upon addition of $PMePh_2$. The reaction of **15** with Me_3SiCl (9 equiv, 80 °C, 24 h) gave $[PhBP_3]Ir(H)_3SiMe_3$[50] (by NMR spectroscopy).

Interestingly, the reactions of **10** and **11** with $LiBHEt_3$ occur at substantially different rates. Reaction of the diiodide **10** with 3 equiv of $LiBHEt_3$ in benzene-d_6 was observed to produce **14a**, and this was followed by the slow, complete conversion to **15** over 36 h. On the other hand, the addition of 3 equiv of $LiBHEt_3$ to the dichloride **11** in benzene-d_6 resulted in rapid and quantitative formation of **15** (<5 min by NMR spectroscopy).

Scheme 3

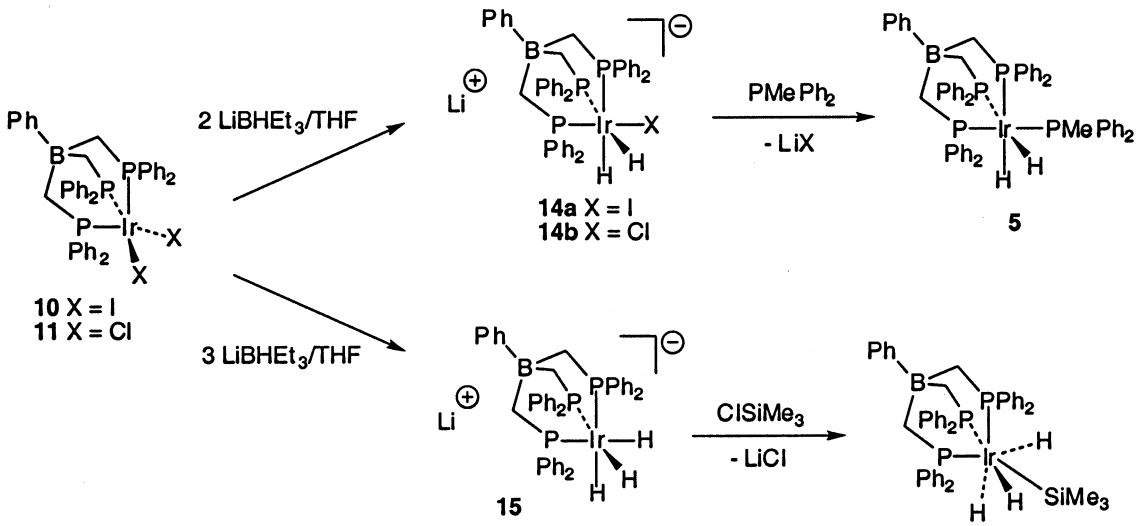

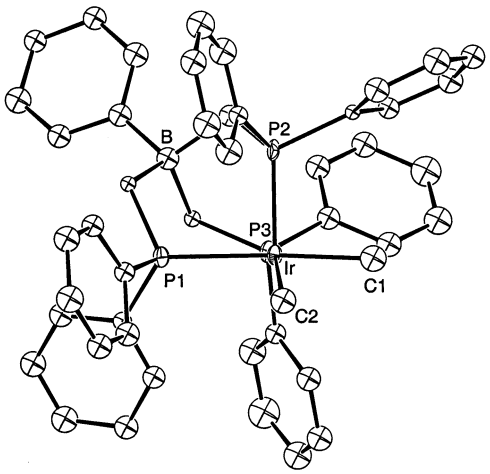

Figure 7. ORTEP diagram of $[PhBP_3]IrMe_2$ (**16**).

Two equivalents of methyllithium (1.4 M in Et_2O) reacted with **10** in benzene to give the pale red dimethyl complex $[PhBP_3]IrMe_2$ (**16**) in 53% isolated yield, as shown in eq 7. Although complex **16** appears to be stable

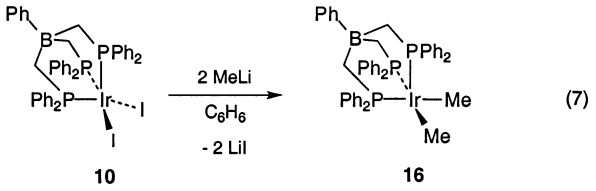

(7)

in solution (65 °C, 2 days, benzene-d_6), it decomposes in the solid state and under vacuum. By ^1H NMR spectroscopy, the methyl groups are equivalent over a wide temperature range (23 to −94 °C, toluene-d_8), and their protons appear as a broad resonance (δ 0.80, benzene-d_6). Likewise, the phosphorus atoms are equivalent by $^{31}P\{^1H\}$ NMR spectroscopy (toluene-d_8, δ −25.3, 23 to −94 °C), suggesting a dynamic structure for **16** in solution.

Crystals of **16** were grown from the slow evaporation of a benzene solution (room temperature), and the solid-state structure was determined by X-ray diffraction (Figure 7; selected bond distances and angles are given in Table 10). The geometry of **16** is intermediate between a square-based pyramid and that of complexes **10** and **13** (pseudo trigonal bipyramidal). Thus, P(1) and C(1) are trans to one another with a P(1)−Ir−C(1) angle of 174.2(6)°. The C(2)−Ir−P(3) angle of 154.2(7)° is between those expected for a square-based pyramid (180°) and a trigonal bipyramid (120°).

Table 10. Selected Bond Distances (Å) and Angles (deg) for 16

(a) Bond Distances			
Ir−P1	2.390(3)	Ir−C1	2.08(1)
Ir−P2	2.218(3)	Ir−C2	2.11(1)
Ir−P3	2.326(4)		
(b) Bond Angles			
P1−Ir−P2	90.2(1)	C1−Ir−P2	92.9(4)
P1−Ir−P3	88.2(1)	C1−Ir−P3	97.2(4)
P2−Ir−P3	87.2(1)	C2−Ir−P1	92.6(4)
C1−Ir−C2	81.3(5)	C2−Ir−P2	118.5(4)
C1−Ir−P1	173.9(4)	C2−Ir−P3	154.3(4)

Discussion

Electronic Properties of $[PhBP_3]Ir$. It has recently been argued by Bergman and co-workers that the Cp* ligand is more electron-donating toward iridium than the Tp^{Me_2} ligand.[2−4] They also suggested that this difference is at least partly responsible for the enhanced reactivity of $Cp^*(PMe_3)Ir(Me)(OTf)$ and $[Cp^*(PMe_3)IrMe]\{B[3,5\text{-}C_6H_3(CF_3)_2]_4\}$ with respect to C−H activation relative to analogous Tp^{Me_2} complexes.[2−4]

The stretching frequencies of metal-bound carbonyls are a gauge of the electron richness of the metal center and thereby of the electron-donating abilities of the ancillary ligands bound to the metal. A comparison of IR data for iridium dicarbonyl complexes of Tp^{Me_2},[51] Cp*,[52] and $[PhBP_3]$ (in hexanes, Table 5) suggests that the relative electron-donating ability of these ligands is $[PhBP_3] \geq Cp^* > Tp^{Me_2}$. A related dicarbonyl complex, $[(triphos)Ir(CO)_2][BF_4]$, prepared by Bianchini and co-workers, has CO stretching frequencies of 2053 and 1954 cm^{-1} (measured as a Nujol mull).[53] This cationic

(51) Ball, R. G.; Ghosh, C. K.; Hoyano, J. K.; McMaster, A. D.; Graham, W. A. G. *Chem. Commun.* **1989**, 341−342.
(52) Hoyano, J. K.; Graham, W. A. G. *J. Am. Chem. Soc.* **1982**, *104*, 3723−3725.
(53) Barbaro, P.; Bianchini, C.; Meli, A.; Peruzzini, M.; Vacca, A.; Vizza, F. *Organometallics* **1991**, *10*, 2227−2238.

complex therefore appears to be less electon-rich than the isoelectronic $[PhBP_3]Ir(CO)_2$.

It is somewhat surprising that the $[PhBP_3]Ir$ and Cp*Ir fragments possess similar electronic properties, given the assumption of cationic character for the metal center in the former system. While CO stretching frequencies provide a reasonable qualitative estimate of the comparative electron richness between a series of structurally related complexes bearing different ligands, it is an approximation. The difference in CO vibrational frequencies between $Cp^*Ir(CO)_2$, $[Tp^{Me_2}]Ir(CO)_2$, and $[PhBP_3]Ir(CO)_2$ may also be a consequence of their different coordination geometries, and to that extent a note of caution must be added in using this gauge to order the relative donor strength of the three ligands.[54]

Since $[PhBP_3]Ir$ appears to be relatively electron-rich, its complexes are expected to be more reactive toward oxidative additions than those of $Tp^{Me_2}Ir$. Indeed, there is a difference between the reactivities of allyl hydride complexes derived from $[PhBP_3]Ir$ and $Tp^{Me_2}Ir$. Whereas **2** readily activates the Si−H bonds of secondary silanes to give silylene complexes of the type $[PhBP_3](H)_2Ir{=}SiR_2$, no reactions were observed[10,50] between silanes and the related complexes $TpIr(H)(\eta^3\text{-}C_8H_{13})$[23] and $Tp^{Me_2}Ir(H)(\eta^3\text{-}C_4H_7)$.[23] This may be due to the enhanced susceptibility of $[PhBP_3]Ir$ complexes toward oxidative additions, though it should be noted that mechanisms involving a change in allyl hapticity (η^3 to η^1) or other ligand dissociation may be responsible for this difference.

Another interesting comparison of related iridium complexes is found in the protonation chemistry of $LIr(PR_3)H_2$ (where L is Tp′, Cp′, or $[PhBP_3]$). The protonation of a variety of $Tp'Ir(PR_3)H_2$ and $Cp'Ir(PR_3)H_2$ complexes has revealed a key difference between the Cp′Ir and Tp′Ir fragments. While $Cp'Ir(PR_3)H_3^+$ complexes are classical hydrides,[35−37] $Tp'Ir(PR_3)(H_2)(H)^+$ complexes are nonclassical hydrides,[38,55] on the basis of T_1(min) NMR data and a neutron diffraction study for $[CpIr(PMe_3)H_3][BF_4]$.[36] For **6**, the T_1(min) value of 281 ± 5 ms indicates that it is the classical hydride complex $\{[PhBP_3]Ir(PMePh_2)H_3\}\{B[3,5\text{-}C_6H_3(CF_3)_2]_4\}$.[56]

One explanation for the difference between these protonated Tp′ and Cp′ complexes is that the more electron-donating Cp′ ligands are better able to support higher oxidation state Ir(V) hydride complexes, whereas Tp′Ir is relatively electron-poor, thus favoring lower valent, nonclassical Ir(III) hydride complexes. An alternative explanation has been put forth suggesting that Tp′ enforces an octahedral geometry at iridium (favoring a six-coordinate, nonclassical hydride complex) while Cp′ is more forgiving with respect to geometry, allowing for a formally seven-coordinate, classical hydride complex.[8,13] However, since $[PhBP_3]$, like Tp′, coordinates in a facial manner and the protonation of **5** gives a classical hydride complex, it seems that the tendency of such complexes to enforce octahedral coordination geometries may be readily overwhelmed by electronic factors.

Coordination Geometries and Steric Considerations for $[PhBP_3]Ir$. The $[PhBP_3]Ir$ complexes reported here exhibit a variety of coordination geometries. In all of the crystallographically characterized complexes with iridium, the $[PhBP_3]$ ligand maintains facial coordination with all P−Ir−P angles close to 90°. Some structures have the expected six-coordinate, octahedral geometry for Ir(III) compounds, including allyls **2** and **3** as well as the highly distorted, cyclometalated tetraphosphine complex **4**.

Perhaps more interesting are the trivalent, five-coordinate structures derived from $[PhBP_3]Ir$. The monomeric nature of the dihalides **10** and **13** was unexpected, given that $[Cp^*Ir(\mu\text{-}X)X]_2$ (X = Cl, Br, I)[57] and $[Tp^{Me_2}Ir(\mu\text{-}Cl)Cl]_2$ [58] complexes are dimeric. Apparently, dimerizations of **10** and **13** are prevented by the significant steric bulk of $[PhBP_3]$. However, dimerization is observed when the halides are replaced with hydride ligands, as $[PhBP_3]IrH_2$ is only observed as the dimer $\{[PhBP_3]Ir(H)(\mu\text{-}H)\}_2$ (**8**). A search of the CSD revealed many examples of trivalent Cp^*IrX_2 complexes (where X_2 is an anionic ligand such as 1,2-dithiobenzene,[59] 1,2-diaminobenzene,[60] or (bis)thiohexafluorobenzene[61]), but for Tp′Ir complexes, which maintain 90° N−Ir−N angles, no such structures are known. Furthermore, with Cp′ and Tp′ ancillary ligands there are no structurally characterized complexes analogous to the five-coordinate dimethyl species **16**.

The stability of 5-coordinate **16** is surprising given that all dimethyl complexes of Cp*Ir contain an additional ligand such as PR_3,[62] CO,[63] or DMSO,[64] and $Tp^{Me_2}IrMe_2(PMe_3)$[65] is the only dimethyl derivative of a Tp′Ir complex. Maitlis and co-workers have shown that methylation of $[Cp^*Ir(\mu\text{-}Cl)Cl]_2$ with Al_2Me_6 leads to formation of a bimetallic methyl-bridged species of the type $[(Cp^*IrMe_3)_2AlMe]$, from which *cis*- and *trans*-$[Cp^*(Me)Ir(\mu\text{-}CH_2)]_2$, as well as Cp^*IrMe_4, are derived.[64,66,67]

While **10** and **13** have pseudo-trigonal-bipyramidal structures (with basal P−Ir−P angles restricted to ca. 90°), $[PhBP_3]IrMe_2$ (**16**) exhibits a distorted-square-pyramidal geometry. This is consistent with the notion that, for d^6 ML_5 complexes, a square-pyramidal geometry is expected, except when π-donor ligands are

(54) As a cautionary point, other comparative carbonyl model studies for complexes supported by (phosphino)borate ligands have shown surprisingly similar CO vibrational energies in comparison to Cp and Tp ligands for structurally related carbonyl complexes: Betley, T. A.; Thomas, J. C.; Peters, J. C. Manuscripts in preparation.

(55) Heinekey, D. M.; Oldham, W. J. *J. Am. Chem. Soc.* **1994**, *116*, 3137−3138.

(56) Crabtree, R. H. *The Organometallic Chemistry of the Transition Metals*, 2nd ed.; Wiley: New York, 1994.

(57) Churchill, M. R.; Julis, S. A. *Inorg. Chem.* **1979**, *18*, 1215−1221.

(58) May, S.; Reinsalu, P.; Powell, J. *Inorg. Chem.* **1980**, *19*, 1582−1589.

(59) Xi, R.; Abe, M.; Suzuki, T.; Nishioka, T.; Isobe, K. *J. Organomet. Chem.* **1997**, *549*, 117−125.

(60) Paek, C.; Ko, J. J.; Uhm, J. K. *Bull. Kor. Chem. Soc.* **1994**, *15*, 980−984.

(61) Garcia, J. J.; Torrens, H.; Adams, H. *J. Chem. Soc., Dalton Trans.* **1993**, *10*, 1529−1536.

(62) Buchanan, J. M.; Stryker, J. M.; Bergman, R. G. *J. Am. Chem. Soc.* **1986**, *108*, 1537−1550.

(63) Isobe, K.; Vazquez de Miguel, A.; Maitlis, P. M. *J. Organomet. Chem.* **1983**, *250*, C25−C27.

(64) de Miguel, A. V.; Gomez, M.; Isobe, K.; Taylor, B. F.; Mann, B. E.; Maitlis, P. M. *Organometallics* **1983**, *2*, 1724−1730.

(65) Tellers, D. M.; Bergman, R. G. *Can. J. Chem.* **2001**, *79*, 525−528.

(66) Isobe, K.; Bailey, P. M.; Maitlis, P. M. *Chem. Commun.* **1981**, 808−809.

(67) de Miguel, A. V.; Isobe, K.; Taylor, B. F.; Nutton, A.; Maitlis, P. M. *J. Chem. Soc., Chem. Commun.* **1982**, 758−759.

Scheme 4

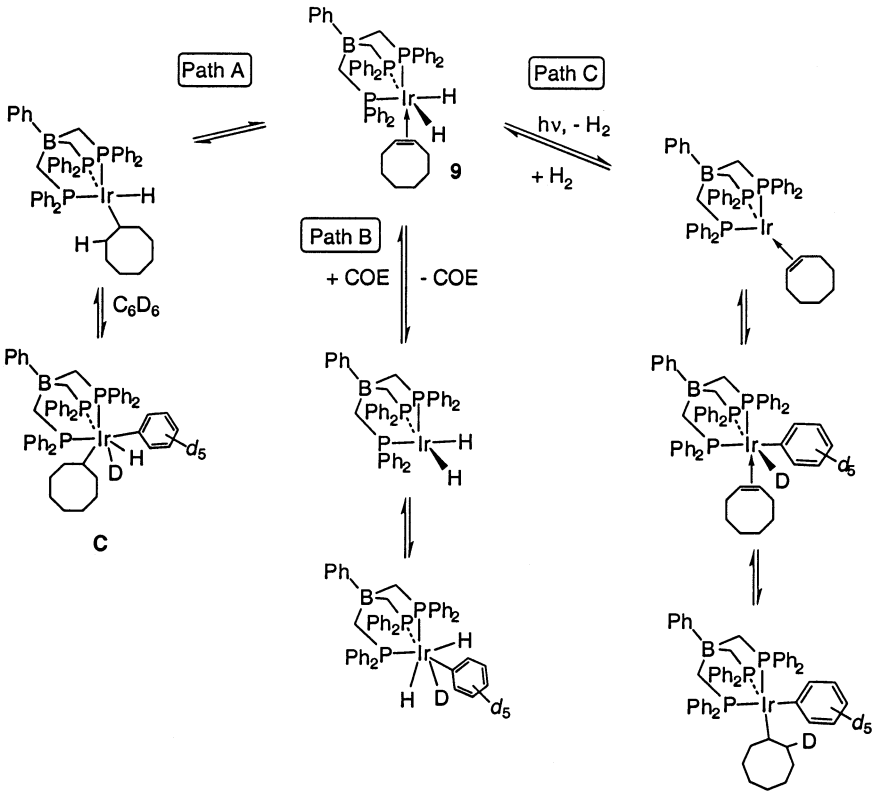

present (as with **10** and **13**).[68,69] In the case with π-donors, a distorted-trigonal-bipyramidal structure is favored, because a π-donor in the equatorial plane can interact with the LUMO on the metal.[70] Interestingly, the only other five-coordinate dialkyl iridium species which have been crystallographically characterized are $R_2Ir[N(SiMe_2CH_2PPh_2)_2]$, where $R_2 = (CH_2Ph)_2$,[71] $(Me)(CH_2CMe_3)$,[72] and $Cp_2Ta(CH_2)_2Ir(CO)_2(PEt_3)$.[73] All three of these have distorted-trigonal-bipyramidal geometries.

For all of the five-coordinate $[PhBP_3]Ir$ complexes (**10**, **11**, **13**, and **16**), only a single ^{31}P NMR resonance is observed over the temperature range of −94 to 23 °C. A dimeric structure of the type $\{[PhBP_3]Ir(X)(\mu\text{-}X)\}_2$ would give rise to two coupled resonances, as would trigonal-bipyramidal or square-based-pyramidal structures. This implies that the solution structures are monomeric and fluxional.

C−H Activation Chemistry. We have observed several examples of intramolecular activation of C−H bonds with $[PhBP_3]Ir$ compounds, beginning with the addition of $[Li(TMED)][PhBP_3]$ to $[(alkene)_2IrCl]_2$ to give allyl complexes **2** and **3** via oxidative addition of coordinated alkene (Scheme 1). The metalation of phenyl substituents on phosphine ligands has also been observed. The photolysis of **5** led to elimination of H_2 and formation of phenyl-metalation products **A** and **B** (eq 3), and the reaction of **2** with PMe_3 gave a similar product, **4** (eq 1). Presumably both of these ligand-activation products form via intermediate, highly reactive, 16-electron species of the type $[PhBP_3]Ir(PR_3)$, which then rapidly undergo ortho metalation of a *P*-phenyl group. For the related compound $Cp^*Ir(PMe_3)H_2$, it has been shown that photolysis generates H_2 and $[Cp^*Ir(PMe_3)]$, which then activates the C−H bonds of numerous alkanes and arenes. Furthermore, intramolecular metalation of a phenyl C−H bond was observed along with benzene activation upon the generation of $[Cp^*Ir(PPh_3)]$.[19]

Although there is no evidence for intermolecular C−H activation in reactions of the $[PhBP_3]Ir$ complexes described above, we have observed chemistry consistent with intermolecular C−D activation of benzene-d_6. While thermolysis of **9** in THF-d_8 led to quantitative formation of COE and dimer **8** (Scheme 2), use of benzene-d_6 as the solvent gave **8** and COE-d_{14} (by ^2H NMR spectroscopy and GC/MS), along with an increased amount of C_6D_5H (by ^1H NMR spectroscopy). It is noteworthy that no partially deuterated COE is produced in this reaction (by GC/MS). Photolysis of **9** (benzene-d_6, 6 h) resulted in loss of COE (undeuterated) to form dimer **8** (ca. 90%) and elimination of H_2 to form the allyl **2** (ca. 10%).

In principle, there are three possible pathways whereby **9** can open a coordination site and activate benzene-d_6. In path A (Scheme 4), migratory insertion followed by oxidative addition of the C−D bond of benzene would give intermediate **C**. In order for COE-d_{14} to be formed exclusively, the rate of reductive elimination of benzene from **C** must be significantly greater than the elimination of cyclooctane (not observed), which seems unlikely. On the other hand, dissociation of COE from **9** would generate $[PhBP_3]IrH_2$, which could then add benzene-

(68) Albright, T. A.; Burdett, J. K.; Whangbo, M.-H. *Orbital Interactions in Chemistry*; Wiley: New York, 1985.
(69) Rossi, A. R.; Hoffmann, R. *Inorg. Chem.* **1975**, *14*, 365.
(70) Thorn, D. L.; Hoffmann, R. *New J. Chem.* **1979**, *3*, 39−45.
(71) Fryzuk, M. D.; MacNeil, P. A.; Massey, R. L.; Ball, R. G. *J. Organomet. Chem.* **1989**, *368*, 231−247.
(72) Fryzuk, M. D.; MacNeil, P. A.; Ball, R. G. *J. Am. Chem. Soc.* **1986**, *108*, 6414−6416.
(73) Hostetler, M. J.; Butts, M. D.; Bergman, R. G. *Inorg. Chim. Acta* **1992**, *200*, 377−392.

d_6 (path B). The resulting partially deuterated complex, **9**-d_x, could undergo migratory insertion to transfer deuterium to COE. In this case, the formation of *only* COE-d_{14} requires that benzene oxidative addition is much faster than dimerization of $[PhBP_3]IrH_2$. A third possibility (path C) involves the reductive elimination of H_2 to give $[PhBP_3]Ir(\eta^2\text{-COE})$, which then activates benzene-d_6 (but does not activate COE to give allyl **2**). Currently, the operative mechanism is not known, but it is interesting to note that a mechanism analogous to path B was suggested in a study of the photolysis of $Tp^{Me_2}Ir(H)_2(COE)$, which gives $Tp^{Me_2}Ir(H)(C_6H_5)P(OMe)_3$ in the presence of $P(OMe)_3$.[74] Attempts to use **9** as an H/D exchange catalyst by heating 10 equiv of COE with **9** in benzene-d_6 gave 3 turnovers of COE-d_{14} (and no partially deuterated COE) before all of the catalyst was irreversibly converted to **8**.

Conclusion

Several iridium complexes featuring the recently introduced tripodal phosphine $PhB(CH_2PPh_2)_3^-$ have been prepared and characterized. These complexes have steric and electronic properties that are distinct from related Cp′Ir and Tp′Ir compounds. It is clear that $[PhBP_3]$ is more sterically encumbering than Cp* and Tp^{Me_2} and is octahedral-enforcing in that it tenaciously maintains 90° P−Ir−P bond angles, even in five-coordinate structures. On the other hand, like Cp*, $[PhBP_3]$ possesses soft donor atoms and yields electron-rich iridium complexes. This is apparent from the spectroscopic comparison of iridium dicarbonyl complexes and from the formation of the classical hydride complex $\{[PhBP_3]Ir(PMePh_2)H_3\}\{B[3,5\text{-}C_6H_3(CF_3)_2]_4\}$ (**6**).

Among the new complexes are allyl hydrides **2** and **3**, from which most of the other compounds are derived, and the synthetically useful dihalides **10** and **11**. Allyl hydride **2** is a versatile starting material, as it serves as a masked source of $[PhBP_3]Ir$ or $[PhBP_3]IrH_2$, depending on the specific reaction conditions employed. This work has demonstrated the tendency of unsaturated, intermediate $[PhBP_3]Ir$ complexes to undergo C−H activation reactions. Although this chemistry has mostly been limited to intramolecular activation of the $[PhBP_3]$ ligand, we have observed catalytic H/D exchange between benzene-d_6 and COE.

Experimental Section

General Considerations. All experiments were performed under dry nitrogen using standard Schlenk or drybox techniques. Ether and THF were distilled under nitrogen from sodium benzophenone ketyl. Dichloromethane, TMED, and acetonitrile were distilled from CaH_2. Toluene was distilled from potassium. To remove olefin impurities, pentane and benzene were pretreated with concentrated H_2SO_4, 0.5 N $KMnO_4$ in 3 M H_2SO_4, $NaHCO_3$, and then anhydrous $MgSO_4$. Benzene-d_6 was distilled from Na/K alloy. $[Ir(COE)_2Cl]_2$ was prepared according to the literature procedure.[75] Carbon monoxide was obtained from Scott Specialty Gases, Inc. Dihydrogen was obtained from Praxair. Other chemicals were obtained from commercial suppliers and used as received. Elemental analyses were performed by the Microanalytical Laboratory in the College of Chemistry at the University of California, Berkeley. FT-infrared spectra were recorded as KBr pellets or as Nujol mulls on a Mattson FTIR 3000 instrument or on a Mattson Infinity FTIR.

NMR Measurements. ^1H, ^{31}P, ^{29}Si, ^{11}B, and ^{13}C NMR spectra were recorded at ambient temperature, unless otherwise noted, on a Bruker DRX-500 instrument equipped with a 5 mm broad-band probe and operating at 500.1 MHz (^1H), 125.8 MHz (^{13}C), 160.46 MHz (^{11}B), 99.4 MHz (^{29}Si), and 202.5 MHz (^{31}P) or on a Bruker AMX-400 with a 5 mm quadranuclear probe at 400.1 MHz (^1H) and 162.0 MHz (^{31}P). Chemical shifts are reported in ppm downfield from $SiMe_4$ and were referenced to solvent peaks (^1H, ^{13}C) or external 85% H_3PO_4 (^{31}P) or external $Et_2O{\cdot}BF_3$ (^{11}B). Bruker XWINNMR software (ver. 2.1) was used for all processing.

X-ray Crystallography. General Considerations. The single-crystal analyses were carried out at the UC Berkeley CHEXRAY crystallographic facility. Measurements were made on a Bruker SMART CCD area detector with graphite-monochromated Mo Kα radiation ($\lambda = 0.710\ 69$ Å). Data were integrated by the program SAINT, corrected for Lorentz and polarization effects, and analyzed for agreement and possible absorption using XPREP. Empirical absorption corrections were made using SADABS. Structures were solved by direct methods and expanded using Fourier techniques. All calculations were performed using the teXsan crystallographic software package. Selected crystal and structure refinement data are summarized in Tables 1 and 7. All crystals were mounted on a glass fiber using Paratone N hydrocarbon oil.

Considerations for 2·THF. The hydrogen atoms on the allyl fragment of the cyclooctene ligand were located in the difference electron density map and their positions refined with fixed thermal parameters. The remaining hydrogens were included in calculated idealized positions but not refined. Except for boron, all non-hydrogen atoms were refined anisotropically.

Considerations for 3·C_6H_6. Except for boron, all non-hydrogen atoms were refined anisotropically; the hydrogen atom positions were calculated but not refined.

Considerations for 4·CH_2Cl_2·C_5H_{12}. With the exception of disordered solvent atoms and boron, all non-hydrogen atoms were refined anisotropically. A dichloromethane molecule was modeled with one isotropic carbon atom, one anisotropic chlorine with full occupancy, a second anisotropic chlorine with 0.83 occupancy, and a third isotropic chlorine with 0.17 occupancy. A second, highly disordered solvent molecule (possibly pentane) was modeled as a number of carbon atoms (some full and some partial occupancy, all refined isotropically) with the following occupancies: C(49), 0.75; C(50), 0.75; C(51), 0.75; C(52), 0.70; C(53), 0.75; C(54), 0.40; C(55), 1.0; C(56), 1.0; C(57), 0.70; C(58), 0.65. These values were obtained by refining the occupancy of these atoms. Hydrogen atom positions were calculated but not refined.

Considerations for 8·C_6H_6. The iridium, phosphorus, and six solvent carbon atoms (C46−C51) were refined anisotropically, and all other non-hydrogen atoms were refined isotropically. Hydrogen atom positions were calculated but not refined.

Considerations for 10·2C_7H_8. The iridium and phosphorus atoms as well as the toluene carbon atoms were refined anisotropically, while the remaining carbon atoms and boron were refined isotropically. The non-toluene carbon atoms were not refined anisotropically. The hydrogen atom positions were calculated but not refined.

Considerations for 13. The iridium, phosphorus, and chlorine atoms were refined anisotropically, the boron and carbon atoms were refined isotropically, and the hydrogen atom positons were calculated but not refined.

(74) Ferrari, A.; Polo, E.; Ruegger, H.; Sostero, S.; Venanzi, L. M. *Inorg. Chem.* **1996**, *35*, 1602−1608.
(75) Herde, J. L.; Lambert, J. C.; Senoff, C. V. *Inorg. Synth.* **1974**, *15*, 18−20.

Considerations for 16. The iridium and phosphorus atoms were refined anisotropically, and the boron and carbon atoms were refined isotropically. The hydrogen atom positions were calculated but not refined.

[Li(TMED)][PhB(CH_2PPh_2)$_3$] (1). A slurry of Li(TMED)-CH_2PPh_2 (12.54 g, 0.039 mol) in 225 mL of Et_2O was stirred and cooled to −78 °C. A toluene (15 mL) solution of $PhBCl_2$ (2.06 g, 0.013 mol) was then added dropwise via cannula. After 3 h, the solution was warmed to room temperature and was stirred for 12 h, giving a colorless precipitate. The solution was filtered, and the precipitate was washed with Et_2O (2 × 25 mL). Phosphine **1** was extracted from the precipitate with ca. 50 °C toluene (2 × 200 mL). The extracts were combined, concentrated, and slowly cooled to −80 °C to give 7.55 g (72%) of colorless, crystalline **1**. ^{1}H NMR (THF-d_8): δ 7.42 (d, 2 H, *o-Ph*B(CH_2PPh_2)$_3$), 7.21 (m, 12 H, PhB(CH_2PPh_2)$_3$), 6.96 (m, 18 H, PhB(CH_2PPh_2)$_3$), 6.63 (m, 2 H, *m-Ph*B(CH_2PPh_2)$_3$), 6.51 (t, 1 H, *p-Ph*B(CH_2PPh_2)$_3$), 2.31 (s, 4 H, $Me_2NCH_2CH_2NMe_2$), 2.16 (s, 12H, $Me_2NCH_2CH_2NMe_2$), 1.23 (br m, 6 H, PhB(CH_2-PPh_2)$_3$). ^{31}P{^{1}H} NMR (THF-d_8): δ −12.4 (s). ^{13}C{^{1}H} NMR (THF-d_8): δ 149.0, 134.9, 134.2, 129.8, 129.0, 127.7, 126.4, 125.6, 121.7 (aryl), 58.9 ($Me_2NCH_2CH_2NMe_2$), 46.4 (Me_2-$NCH_2CH_2NMe_2$). ^{11}B NMR (C_6D_6): δ −14.0 (s). Anal. Calcd for $C_{51}H_{57}BLiN_2P_3$: C, 75.75; H, 7.10. Found: C, 75.43; H, 6.91.

[$PhBP_3$]Ir(η^3-C_8H_{13})H (2). A stirred slurry of $[(COE)_2IrCl]_2$ (1.09 g, 1.21 mmol) in benzene (15 mL) was added to a stirred slurry of **1** (1.96 g, 2.42 mmol) in benzene (35 mL) to give a dark green solution. After 15 h, all solvent was removed in vacuo and the resulting tan/green solid was washed with pentane (2 × 10 mL). Complex **2** was then extracted with 40 °C benzene and crystallized from toluene in three crops (87% yield). ^{1}H NMR (benzene-d_6): δ 8.10 (d, 2 H, *o-Ph*B(CH_2PPh_2)$_3$), 7.8−6.7 (m, 30 H, PhB(CH_2PPh_2)$_3$), 7.65 (m, 2 H, *m-Ph*B(CH_2-PPh_2)$_3$), 7.41 (t, 1 H, *p-Ph*B(CH_2PPh_2)$_3$), 4.90 (m, 1 H, C*H*), 3.57 (m, 2 H, C*H*), 3.13 (m, 2 H, CH_2), 2.78 (m, 2 H, CH_2), 2.03 (m, 2 H, PhB(CH'_2PPh_2)(CH_2PPh_2)$_2$), 1.88 (m, 4 H, PhB-(CH'_2PPh_2)(CH_2PPh_2)$_2$), 1.35 (m, 5 H, CH_2), −12.55 (dt, $^2J_{HP(trans)}$ = 150 Hz, $^2J_{HP(cis)}$ = 14 Hz, 1 H, Ir*H*). ^{31}P{^{1}H} NMR (benzene-d_6): δ −7.77 (d, $^2J_{PP}$ = 22 Hz), −13.37 (br). ^{13}C{^{1}H} NMR (THF-d_8): δ 133.2, 133.1, 132.8, 132.0, 129.2, 128.9, 124.8 (aryl), 93.2 (H*C*[(CH)$_2$(CH_2)$_5$)]), 56.9 (HC[(*C*H)$_2$(CH_2)$_5$)]), 39.1 (HC[(CH)$_2$(*C*H_2)$_5$)]), 30.7 (HC[(CH)$_2$(*C*H_2)$_5$)]), 26.0 (HC-[(CH)$_2$(*C*H_2)$_5$)]). ^{11}B NMR (C_6D_6): δ −12.0 (s). IR (Nujol, cm^{-1}): 2143 m (IrH). Anal. Calcd for $C_{53}H_{55}BIrP_3$: C, 64.43; H, 5.61. Found: C, 64.33; H, 5.51.

[$PhBP_3$]Ir(η^3-C_3H_5)H (3). A thick-walled 250 mL flask fitted with a PTFE stopcock was charged with $[(COE)_2IrCl]_2$ (0.691 g, 0.771 mmol), a magnetic stir bar, and 75 mL of THF. The orange solution was cooled to −78 °C with a dry ice/acetone bath and degassed in vacuo. Propene (1 atm) was introduced and allowed to saturate the solution for 2 min, at which point the flask was cooled with liquid nitrogen to give a frozen yellow solution. [Li(TMED)][PhB(CH_2PPh_2)$_3$] (1.250 g, 1.55 mmol) was dissolved in 25 mL of THF and added to the frozen solution, which was then warmed to room temperature and was stirred for 24 h. Solvent was removed in vacuo, and the solid residue was triturated with pentane (3 × 10 mL). The product was extracted with benzene (2 × 30 mL) and recrystallized from THF at −80 °C to give 1.028 g (72%) of colorless, crystalline **3** in three crops. ^{1}H NMR (benzene-d_6): δ 8.09 (d, J = 7 Hz, 2 H, *o-Ph*B(CH_2PPh_2)$_3$), 7.8−6.7 (m, 30 H, PhB(CH_2PPh_2)$_3$), 7.65 (m, 2 H, *m-Ph*B(CH_2PPh_2)$_3$), 7.41 (t, J = 7 Hz, 1 H, *p-Ph*B(CH_2PPh_2)$_3$), 4.17 (m, 1 H, *H*C(CHH′)$_2$), 3.26 (m, 2 H, HC(C*H*H′)$_2$), 2.23 (d, J = 6 Hz, 2 H, HC(CH*H*′)$_2$). 2.0−1.84 (m, 6 H, PhB(CH_2PPh_2)), −12.79 (dt, $^2J_{HP(trans)}$ = 135 Hz, $^2J_{HP(cis)}$ = 13, Hz 1 H, Ir*H*). ^{31}P{^{1}H} NMR (benzene-d_6): δ −7.83 (d, J_{pp} = 21 Hz, 2 P), −16.67 (t, 1 P). ^{13}C{^{1}H} NMR (benzene-d_6): δ 132.3, 132.2, 132.1, 132.0, 131.1, 131.0, 128.7, 124.0 (aryl), 92.9 (H*C*(CH_2)$_2$), 33.7 (HC(*C*H_2)$_2$), 14.1 (br PhB-(*C*H_2PPh$_2$)). ^{11}B NMR (C_6D_6): δ −12.4 (s). IR (benzene, cm^{-1}): 2148 m (IrH). Anal. Calcd for $C_{48}H_{47}BIrP_3$: C, 62.68; H, 5.15. Found: C, 62.51; H, 5.55. Mp: 257−260 °C dec.

{PhB[(CH_2PPh_2)$_2$($CH_2PPhC_6H_4$)]}Ir(H)(PMe_3) (4). A thick-walled 100 mL flask fitted with a PTFE stopcock was charged with **3** (0.143 g, 0.145 mmol), a magnetic stir bar, and 4 mL of benzene. Addition of PMe_3 (22 μL, 0.21 mmol) via syringe resulted in complete dissolution of the iridium compound. The flask was placed in an oil bath maintained at 55 °C for 2.5 days. A small amount of solid was removed by filtration, and the solvent was removed under vacuum. Crystallization from CH_2Cl_2 at −35 °C gave 0.127 g (92%) of spectroscopically pure **4**·2CH_2Cl_2. ^{1}H NMR (CD_2Cl_2): δ 7.92, 7.73, 7.58, 7.42, 7.32, 7.26−7.10, 7.04, 6.90, 6.84, 6.65, 6.34 (aryl), 2.37 (m, 1 H, BC*H*H′), 2.20 (m, 1 H, BCH*H*′), 1.71 (d, $^3J_{HP}$ = 9 Hz, 9 H, PMe_3), −9.47 (dm, $^2J_{HP(trans)}$ = 121 Hz, 1 H, Ir*H*). ^{31}P{^{1}H} NMR (CD_2Cl_2): δ −3.13 (pseudo q, $2J_{PP(cis)}$ = 18 Hz), −19.94 (m), −58.26 (ddd, $^2J_{PP(trans)}$ = 283 Hz, $^2J_{PP(cis)}$ = 21 Hz, $^2J'_{PP(cis)}$ = 16 Hz), −69.90 (ddd, $^2J_{PP(trans)}$ = 283 Hz, $^2J_{PP(cis)}$ = 26 Hz, $^2J'_{PP(cis)}$ = 17 Hz). ^{13}C{^{1}H} NMR (CD_2Cl_2): δ 157.1, 142.9, 142.2, 141.9, 135.3, 134.2, 134.1, 133.4, 133.3, 133.1, 132.4, 132.2, 130.6, 130.0, 129.5, 128.8, 128.0, 127.9, 127.6, 127.4, 124.1, 122.2 (aryl), 25.3 (br m, BCH_2P), 23.5 (br m, BCH_2P), 22.8 (dm, J = 32 Hz, PCH_3), 9.8 (br m, BCH_2P). IR (KBr, cm^{-1}): 3045 br m, 3002 w, 2908 w, 2882 w, 2077 br m (IrH), 1480 m ([$PhBP_3$]), 1433 s ([$PhBP_3$]), 1089 m, 951 m, 921 m, 848 w, 735 s, 695 s, 514 s, 496 w, 444 w. Anal. Calcd for **4**·2CH_2Cl_2 ($C_{50}H_{54}BIrP_4Cl_4$): C, 53.44; H, 4.84. Found: C, 53.72; H, 4.80. Mp: 260−262 °C.

[$PhBP_3$]Ir($PMePh_2$)H_2 (5). A thick-walled 100 mL flask fitted with a PTFE stopcock was charged with **3** (0.168 g, 0.170 mmol), $PMePh_2$ (0.036 g, 0.180 mmol), a magnetic stir bar, and 3 mL of benzene. The solution was stirred and heated to 80 °C for 24 h, during which time the solution turned red. Volatile materials were removed in vacuo, and off-white **5** was recrystallized in 46% yield via diffusion of pentane into a THF solution of **5**. ^{1}H NMR (benzene-d_6): δ 8.23 (d, J = 10 Hz, 2 H, *o-Ph*B(CH_2PPh_2)$_3$), 7.9−6.7 (m, 43 H, remaining [$PhBP_3$] aryl, Me*PPh*$_2$), 2.38−2.09 (m, 4 H, BCH_2P trans to H), 1.73 (d, $^2J_{HP}$ = 17 Hz, 2 H, BCH_2P trans to $PMePh_2$), 0.51 (dd, $^2J_{HP}$ = 8 Hz, $^4J_{HP}$ = 2 Hz, 3 H, PCH_3Ph_2), −11.04 (dm, $^2J_{HP}$ = 107 Hz, 2 H, IrH_2). ^{31}P{^{1}H} NMR (benzene-d_6): δ −0.98 (dt, $^2J_{PP(trans)}$ = 285 Hz, $^2J_{PP(cis)}$ = 21 Hz, 1 P, [$PhBP_3$] trans to $PMePh_2$), −10.42 (t, $^2J_{PP(cis)}$ = 21 Hz, 2 P, [$PhBP_3$] trans to H), −16.84 (dt, $^2J_{PP(trans)}$ = 285 Hz, $^2J_{PP(cis)}$ = 21 Hz, 1 P, $PMePh_2$). ^{13}C-{^{1}H} NMR (THF-d_8): δ 144.7 143.1, 141.1, 139.6, 134.5, 133.4, 132.9, 132.7, 130.1, 129.3, 129.2, 128.8, 128.6, 128.1, 127.9, 123.9 (aryl), 20.8 (br, BCH_2P), 11.5 (d, $^1J_{CP}$ = 27 Hz, P*Me*Ph_2). IR (KBr, cm^{-1}): 3055 br m, 2990 br m, 2979 br m, 2157 br m (IrH), 2053 s (IrH), 1482 m ([$PhBP_3$]), 1433 s ([$PhBP_3$]), 1089 s, 922 m, 887 s, 849 w, 738 s, 699 s, 595 w, 514 s, 481 s, 416 w. Anal. Calcd for $C_{58}H_{54}BIrP_4$: C, 60.17; H, 5.05. Found: C, 60.23; H, 4.92. Mp: 160−164 °C dec.

Photolysis of 5. A Pyrex, PTFE-capped NMR tube containing 0.5 mL of a benzene-d_6 solution of **5** (0.010 g, 0.093 mmol) was irradiated under N_2 in a Rayonet photolysis apparatus for 13 h, during which time the conversion to metalation products (ultimately **A** and **B** in a 2:5 ratio) was monitored by NMR spectroscopy. The structure assignments are based on comparisons of ^{1}H and ^{31}P{^{1}H} NMR data to those of metalation product **4**. Although complete assignment of the ^{1}H NMR spectrum was not possible, due to the presence of many overlapping resonances in the methylene region (δ 1.40−2.44; 12 inequivalent BC*HH*′P resonances for **A** + **B**) and in the aryl region (δ 6.30−7.75; 56 inequivalent aryl resonances for **A** + **B**), the PCH_3 and Ir*H* resonances were readily identified. Data for **A** are as follows. ^{1}H NMR (benzene-d_6): δ 0.87 (dd, $^2J_{HP}$ = 10 Hz, $^4J_{HP}$ = 3 Hz, 3 H, PCH_3Ph_2), −9.03 (dm, $^3J_{HP(trans)}$ = 119 Hz, 1 H, Ir*H*). ^{31}P{^{1}H} NMR (benzene-d_6): δ −3.81 (dt, $^2J_{PP(trans)}$ = 306 Hz, $^2J_{PP(cis)}$ = 21 Hz), −16.18 (q, $^2J_{PP(cis)}$ = 18 Hz), −25.59 (q, $^2J_{PP(cis)}$ = 17 Hz), −98.30 (dt, $^2J_{PP(trans)}$ = 305

Hz, $^2J_{PP(cis)}$ = 18 Hz). Data for **B** are as follows. ^{1}H NMR (benzene-d_6): δ 1.95 (dd, $^2J_{HP}$ = 8 Hz, $^4J_{HP}$ = 2 Hz, 3 H, PCH_3-Ph$_2$), −9.31 (dm, $^3J_{HP(trans)}$ = 289 Hz, 1 H, IrH). ^{31}P{^{1}H} NMR (benzene-d_6): δ −6.91 (dt, $^2J_{PP(trans)}$ = 309 Hz, $^2J_{PP(cis)}$ = 21 Hz), −9.81 (q, $^2J_{PP(cis)}$ = 19 Hz), −24.89 (q, $^2J_{PP(cis)}$ = 20 Hz), −104.87 (dt, $^2J_{PP(trans)}$ = 311 Hz, $^2J_{PP(cis)}$ = 20 Hz).

Observation of {[PhBP$_3$]Ir(PMePh$_2$)H$_3$}{B[3,5-C$_6$H$_3$(CF$_3$)$_2$]$_4$} (6). Compound **5** (0.0078 g, 0.0072 mmol) was dissolved in 0.5 mL of CD_2Cl_2 to give a colorless solution. To this solution was added [H(OEt$_2$)$_2$]{B[3,5-C$_6$H$_3$(CF$_3$)$_2$]$_4$} (0.0071 g, 0.0071 mmol), which gave an orange solution. In a PTFE-sealed NMR tube a variable-temperature T_1(min) determination was carried out on the IrH resonance of **6** using the null method on a Bruker DRX-500 instrument. The T_1(min) value for the IrH resonance of **6** was determined to be 281 ± 5 ms at 255 K. Similarly, the T_1(min) value for the IrH resonance of **5** was determined to be 274 ± 5 ms at 245 K in CD_2Cl_2. ^{1}H NMR (CD_2Cl_2): δ 7.73, 7.57, 7.36, 7.29, 6.95, 6.86 (aryl), 2.06 (br, 2 H, BCH_2P), 1.91 (br, 4 H, BCH_2P), 0.53 (d, $^2J_{HP}$ = 9 Hz, 3 H, PMePh$_2$), −11.21 (dm, $^2J_{HP}$ = 112 Hz, 4 H, IrH_3). ^{31}P{^{1}H} NMR (CD_2Cl_2): δ −6.20 (br d, $^2J_{PP(trans)}$ = 286 Hz, 1 P, BPP$_2$ trans to PMePh$_2$), −14.76 (br, 2 P, BPP'_2), −19.23 (dt, $^2J_{PP(trans)}$ = 286 Hz, $^2J_{PP(cis)}$ = 19 Hz, 1 P, PMePh$_2$).

[PhBP$_3$]Ir(CO)$_2$ (7). A thick-walled 100 mL flask fitted with a PTFE stopcock was charged with **3** (0.125 g, 0.136 mmol), a magnetic stir bar, and 4 mL of benzene. The colorless solution was then degassed with two freeze−pump−thaw cycles, and carbon monoxide (1 atm) was introduced. The solution was heated at 80 °C for 5 days, during which time it turned yellow. Solvent was removed in vacuo, and the resulting solid was washed with pentane (3 mL) and dried under vacuum. Compound **7** was isolated as a pale yellow solid (0.091 g, 72%). ^{1}H NMR (benzene-d_6): δ 8.05 (d, J = 7 Hz, 2 H, o-PhB(CH$_2$PPh$_2$)$_3$), 7.65 (m, 2 H, m-PhB(CH$_2$PPh$_2$)$_3$), 7.40 (m, 13 H, aryl), 6.78 (m, 18 H, aryl), 1.84 (br d, $^3J_{HP}$ = 11 Hz, 6 H, PhB(CH_2PPh$_2$)). ^{31}P{^{1}H} NMR (benzene-d_6): δ −10.59 (s). ^{13}C{^{1}H} NMR (benzene-d_6): δ 187.9 (q, $^2J_{CP}$ = 24 Hz, CO), 138.6, 132.7, 129.8, 129.1, 126.3, 125.3 (aryl), 14.7 (br) PhB(CH_2PPh$_2$). ^{11}B NMR (C_6D_6): δ −11.7 (s). IR (hexanes, cm^{-1}): 3050 br w, 2905 br w, 2024 s (CO), 1940 s (CO), 1481 w ([PhBP$_3$]), 1434 m ([PhBP$_3$]), 1160 w, 1091 m, 917 w, 740 m, 696 s, 551 w, 515 s, 481 w, 438 w. Anal. Calcd for C$_{47}$H$_{41}$BIrP$_3$: C, 60.45; H, 4.43. Found: C, 60.30; H, 4.70. Mp: 256−260 °C dec.

{[PhBP$_3$]Ir(μ-H)(H)}$_2$ (8). An NMR tube fitted with a PTFE valve was charged with **3** (0.025 g, 0.027 mmol) and ca. 0.6 mL of benzene-d_6. After two freeze−pump−thaw cycles, 1 atm of H_2 was introduced. The NMR tube was heated to 80 °C for 2 days, during which time orange crystals grew at the bottom of the tube. Crystalline **8** was isolated in 75% yield (0.018 g). IR (KBr, cm^{-1}): 2114 (terminal IrH), 1088 (bridging IrH). Anal. Calcd for C$_{90}$H$_{88}$P$_6$Ir$_2$B$_2$: C, 61.36; H, 5.03. Found: C, 61.46; H, 4.96. Mp: >260 °C.

[PhBP$_3$]Ir(H)$_2$(COE) (9). A 5 mL THF solution of **2** (0.098 g, 0.099 mmol) and COE (0.035 g, 0.31 mmol) in a PTFE-sealed vessel was degassed with three freeze−pump−thaw cycles, and 1 atm of H_2 was introduced. Over the 11.5 h of reaction time the solution became pale orange, and a small amount of crystalline **8** formed (by IR spectroscopy). The solution was filtered through fine glass fiber filter paper, and the solvent was removed in vacuo, giving off-white **9** (0.058 g, 59%). ^{1}H NMR (THF-d_8): δ 7.69 (m, 8 H, aryl), 7.0−7.23 (m, 18 H, aryl), 6.80 (m, 4 H, aryl), 3.78 (br, 2 H, COE CH), 2.45 (m, 2 H, CH_2), 2.19 (m, 2 H, CH_2), 1.65 (m, 6 H, CH_2), 1.48 (m, 4 H, CH_2), 1.31 (m, 2 H, CH_2), 0.94 (m, 2 H, CH_2). ^{31}P{^{1}H} NMR (THF-d_8): δ 2.07 (t, 1 P, $^2J_{PP(cis)}$ = 21 Hz), 13.12 (d, 2 P, $^2J_{PP(cis)}$ = 21 Hz). ^{13}C{^{1}H} NMR (CD_2Cl_2): δ 133.9, 132.2, 131.8, 129.4, 129.2, 128.9, 128.5, 128.1, 127.7, 127.6, 125.6, 124.0 (aryl), 73.1 (d, $^2J_{CP(trans)}$ = 9 Hz, COE CH), 34.3 (s, CH_2), 33.9 (s, CH_2), 26.5 (s, CH_2). IR (KBr, cm^{-1}): 3053 m, 2918 m, 2845 w, 2108 br m (IrH), 2034 br w (IrH), 1481 m ([PhBP$_3$]), 1433 s ([PhBP$_3$]), 1261 w, 1159 w, 1091 s, 1027 w, 926 m, 861 w, 806 w, 741 s, 695 s, 515 s, 481 w. Anal. Calcd for C$_{53}$H$_{57}$IrP$_3$B: C, 64.29; H, 5.80. Found: C, 64.55; H, 6.05. Mp: 187−188 °C dec.

[PhBP$_3$]IrI$_2$ (10). Allyl **2** (0.532 g, 0.538 mmol) was stirred in 8 mL of 3:2 benzene/acetonitrile (15 mL) for 20 min to give a colorless solution. A 7 mL solution of I_2 in benzene was added to the solution of **2**, generating a blood red solution of **10**. The solvent was removed in vacuo, and the dark purple crystalline product was washed with pentane (3 × 10 mL) to aid in COE removal, yielding **10** in 94% yield (0.569 g). X-ray-quality crystals were grown from a concentrated toluene solution at −35 °C. ^{1}H NMR (benzene-d_6): δ 7.94 (d, J = 7 Hz, 2 H, o-PhB(CH$_2$PPh$_2$)$_3$), 7.63 (m, 2 H, m-PhB(CH$_2$PPh$_2$)$_3$), 7.55 (m, 12 H, PhB(CH$_2$PPh_2)$_3$), 7.41 (t, J = 7 Hz, 1 H, p-PhB(CH$_2$PPh$_2$)$_3$), 6.83 (m, 6 H, PhB(CH$_2$PPh_2)$_3$), 6.69 (m, 12 H, PhB(CH$_2$PPh_2)$_3$), 1.91 (br d, $^2J_{HP}$ = 10 Hz, 6 H, PhB(CH_2PPh$_2$)$_3$). ^{31}P{^{1}H} NMR (benzene-d_6): δ 4.34 (s). ^{13}C{^{1}H} NMR (CD_2Cl_2): δ 134.0, 133.7, 132.1, 130.9, 128.4, 128.21 (aryl), 14.46 (br, PhB(CH_2PPh$_2$)$_3$). ^{11}B NMR (C_6D_6): δ −9.8 (s). IR (KBr, cm^{-1}): 2920 m, 2656 s, 2448 w, 1481 m ([PhBP$_3$]), 1434 s ([PhBP$_3$]), 1160 w, 994 w, 971 w, 925 w, 863 w, 740 m, 693 s, 514 s, 485 w, 445 w. Anal. Calcd for C$_{45}$H$_{41}$BIrP$_3$I$_2$: C, 47.76; H, 3.65. Found: C, 48.13; H, 4.15. Mp: 252−260 °C (238 °C dec).

[PhBP$_3$]IrCl$_2$ (11). Allyl **3** (0.453 g, 0.492 mmol) was dissolved in 9 mL of 7:3 benzene/carbon tetrachloride. This solution was stirred in a PTFE-sealed vessel at 65−70 °C for 7.5 days, over which time the solution turned orange. Note that higher temperatures lead to formation of the chloroborate **12**. This reaction is readily monitored by ^{31}P{^{1}H} NMR spectroscopy to ensure that conversion of **3** to **11** occurs cleanly. When the mixture was cooled to room temperature, orange crystals deposited on the sides of the flask (0.093 g). The remaining product was isolated as an orange powder (0.451 g) by removing solvent in vacuo and washing the resulting solid with pentane (3 × 15 mL). Total yield: 97%. ^{1}H NMR (benzene-d_6): δ 7.96 (d, J = 7 Hz, 2 H, o-PhB(CH$_2$PPh$_2$)$_3$), 7.64 (m 15 H, m-PhB(CH$_2$PPh_2)$_3$), 7.44 (t, J = 7 Hz, 1 H, p-PhB(CH$_2$PPh$_2$)$_3$), 6.78 (m, 6 H, PhB(CH$_2$PPh_2)$_3$), 6.66 (m, 12 H, PhB(CH$_2$PPh_2)$_3$), 1.82 (br d, $^2J_{HP}$ = 9 Hz, 6 H, PhB(CH_2PPh$_2$)$_3$). ^{31}P{^{1}H} NMR (benzene-d_6): δ 4.92 (s). ^{13}C{^{1}H} NMR (CD_2Cl_2): δ 133.5, 132.2, 131.0, 128.5, 128.2, 125.3 (aryl), 12.9 (br, PhB(CH_2PPh$_2$)$_3$). ^{11}B NMR (C_6D_6): δ −9.7 (s). IR (KBr, cm^{-1}): 3055 br m, 1478 m ([PhBP$_3$]), 1434 s ([PhBP$_3$]), 1160 m, 1089 s, 917 m, 741 s, 694 s, 684 s, 483 m, 440 w. Anal. Calcd for C$_{45}$H$_{41}$BIrP$_3$Cl$_2$: C, 56.97; H, 4.36. Found: C, 56.76; H, 4.51. Mp: >260 °C.

Observation of [PhBP$_3$]Ir(COE)(MeCN) (12). Complex **12** forms upon dissolving **2** in benzene-d_6/CD_3CN, and it is converted back to **2** upon solvent removal in vacuo. ^{1}H NMR (benzene-d_6/CD_3CN): δ 7.78 (m, 6 H, aryl), 7.31 (t, J = 7 Hz, 3 H, aryl), 7.08−6.60 (multiplets, 26 H, aryl), 2.61 (br d, J = 13 Hz, 2 H, vinyl CH) 1.99−1.40 (overlapping multiplets, 18 H, CH_2). ^{31}P{^{1}H} NMR (benzene-d_6/CD_3CN): δ −8.36 (d, J_{PP} = 23 Hz, 2 P), −15.69 (t, J_{PP} = 23 Hz, 1 P).

[ClB(CH$_2$PPh$_2$)$_3$]IrCl$_2$ (13). In a flask fitted with a PTFE stopcock, allyl **2** (0.091 g, 0.092 mmol) was dissolved in 4 mL of benzene/CCl_4 (1:1), and the resulting solution was heated at 105 °C. Over the reaction time of 10 days, orange crystals of **13** formed above the solvent miniscus. The crystals were isolated by decanting the solvent and were dried in vacuo to give **13** in 24% yield. ^{1}H NMR (CD_2Cl_2): δ 7.45 (br, 12 H, ClB(CH$_2$PPh_2)$_3$), 7.27 (m, 6 H, ClB(CH$_2$PPh_2)$_3$), 7.08 (m, 12 H, ClB(CH$_2$PPh_2)$_3$), 1.89 (br d, $^2J_{HP}$ = 10 Hz, 6 H, PhB(CH$_2$PPh$_2$)$_3$). ^{31}P{^{1}H} NMR (benzene-d_6): δ 0.93 (s). ^{13}C{^{1}H} NMR (CD_2Cl_2): δ 133.3, 131.1, 128.4, 15.6 (br, PhB(CH$_2$PPh$_2$)$_3$). ^{11}B NMR (C_6D_6): δ −8.7 (s). IR (KBr, cm^{-1}): 3056 br m, 1484 m ([PhBP$_3$]), 1434 s ([PhBP$_3$]), 1136 m, 1091 s, 942 m, 815 m, 741 m, 689 s, 517 s, 487 m, 442 m. Anal. Calcd for C$_{39}$H$_{36}$BIrP$_3$Cl$_3$: C, 51.64; H, 4.00. Found: C, 51.47; H, 4.05. Mp: >260 °C.

Observation of [Li(THF)$_n$]{[PhBP$_3$]Ir(H)$_2$I} (14a). Compound **10** (0.020 g, 0.018 mmol) was dissolved in 0.5 mL of benzene-d_6, and LiBHEt$_3$ (1.0 M in THF, 34 μL, 0.034 mmol) was then added via syringe. Upon addition the purple solution turned pale orange and a fine white precipitate formed. The solution was filtered through glass fiber filter paper and analyzed by NMR spectroscopy. Solvent removal in vacuo resulted in decomposition of **14a** to several species. However, **14a** was characterized by derivatization: thermolysis with PMePh$_2$ (13 equiv, room temperature, benzene-d_6, 5.5 h) gave [PhBP$_3$]Ir(PMePh$_2$)H$_2$ (**5**; by NMR spectroscopy). ^{1}H NMR (benzene-d_6): δ 8.02 (q, J = 8 Hz, 6 H, aryl), 7.65 (t, J = 6 Hz, 5 H, aryl), 7.59 (t, J = 7 Hz, 1 H, aryl), 7.42 (m, 6 H, aryl), 7.00 (m, 4 H, aryl), 6.89 (m, 6 H, aryl), 6.80 (t, J = 7 Hz, 2 H), 6.72 (m, 5 H, aryl), −12.11 (dm, $^2J_{HP}$ = 111 Hz, 2 H, Ir*H*). ^{31}P{^{1}H} NMR(benzene-d_6): δ 7.9 (t, $^2J_{PP}$ = 11 Hz, 1 P), −17.7 (d, $^2J_{PP}$ = 11 Hz, 2 P). ^{11}B NMR (C$_6$D$_6$): δ −11.8 (s).

Observation of [Li(THF)$_n$]{[PhBP$_3$]Ir(H)$_2$Cl} (14b). Complex **14b** was observed with a mixture of hydride products (including **15**) upon the addition of LiBHEt$_3$ (1.0 M in THF, 17 μL, 0.017 mmol) to a 0.5 mL benzene-d_6 solution of **11** (0.008 g, 0.009 mmol). It decomposed upon removing the solvent in vacuo. Its ^{1}H NMR spectrum resembles that of **14a** but is obscured by the presence of other species. Its IrH resonance was observed at δ −10.12 (dm, $^2J_{HP(trans)}$ = 125 Hz). ^{31}P{^{1}H} NMR (benzene-d_6): δ 9.1 (t, $^2J_{PP}$ = 14 Hz, 1 P) and δ −9.2, (d, $^2J_{PP}$ = 14 Hz, 2 P). ^{11}B NMR (C$_6$D$_6$): δ −11.2 (s).

Observation of [Li(THF)$_n$]{[PhBP$_3$]IrH$_3$} (15). To a 0.5 mL benzene-d_6 solution of **11** (0.008 g, 0.009 mmol) was added LiBHEt$_3$ (1.0 M in THF, 24 μL, 0.024 mmol). Like **14a** and **14b**, this complex decomposed upon solvent removal. It was characterized by derivatization by reaction with Me$_3$SiCl (9 equiv, 80 °C, 24 h), giving [PhBP$_3$]Ir(H)$_3$SiMe$_3$[50] (by ^{31}P{^{1}H} NMR spectroscopy). ^{1}H NMR (benzene-d_6): δ 8.18 (d, J = 7 Hz, 2 H, aryl), 7.64 (m, 13 H, aryl), 7.51 (m, 6 H, aryl), 7.69 (t, J = 7 Hz, 2 H, aryl), 6.88 (m, 12 H, aryl), 1.89 (m, 6 H, BCH_2P), −12.42 (dm, $^2J_{HP(trans)}$ = 96 Hz, 3 H, Ir*H*). ^{31}P{^{1}H} NMR (benzene-d_6): δ 1.40 (s). ^{11}B NMR (C$_6$D$_6$): δ −12.1 (s).

[PhBP$_3$]IrMe$_2$ (16). Dropwise addition of methyllithium (1.6 M in Et$_2$O, 228 μL, 0.365 mmol) to a stirred solution of **10** (0.206 g, 0.182 mmol) in 20 mL of benzene resulted in a color change from dark red to pale orange, and a colorless precipitate formed. The solvent was removed under reduced pressure, but the resulting solid was kept under vacuum only briefly (15 min) in order to prevent decomposition. The solid was washed with pentane (10 mL), and compound **16** was extracted into benzene (15 mL). This extract was concentrated to 5 mL and layered with pentane to give 0.088 g (53%) of the product. Complex **16** is unstable in the solid state at room temperature and under vacuum; thus, elemental analyses were consistently off by 1−2%. ^{1}H NMR (benzene-d_6/THF-d_8, 9:1): δ 8.06 (d, J = 7 Hz, 2 H, *o*-*Ph*B(CH$_2$PPh$_2$)$_3$), 7.71 (m, 12 H, PhB(CH$_2$P*Ph*$_2$)$_3$), 7.50 (t, J = 7 Hz, 1 H, *p*-*Ph*B(CH$_2$PPh$_2$)$_3$), 7.00 (m, 18 H, PhB(CH$_2$P*Ph*$_2$)$_3$), 6.83 (m, 2 H), 2.07 (br, 6 H, PhB(C*H*$_2$PPh$_2$)$_3$), 0.80 (br, 6 H, IrC*H*$_3$). ^{31}P{^{1}H} NMR (benzene-d_6/THF-d_8, 9:1): δ −25.3 (s). ^{13}C{^{1}H} NMR (CD$_2$Cl$_2$): δ 142.8, 133.9, 126.7, 126.5, 122.6 (aryl), 18.7 (br, B*C*H$_2$), −3.5 (dm, $^1J_{CP(trans)}$ = 92 Hz, Ir*C*H$_3$). ^{11}B NMR (C$_6$D$_6$): δ −10.6 (s). Mp: 84−89 °C dec.

Acknowledgment is made to the National Science Foundation for their generous support of this work. We thank Dr. Fred Hollander of the UC Berkeley CHEXRAY facility for assistance with the X-ray structure determinations and for solving the structure of **2**.

Supporting Information Available: Tables of bond distances and angles and anisotropic displacement parameters for **2**−**4**, **8**, **10**, **13**, and **16**. This material is available free of charge via the Internet at http://pubs.acs.org.

OM0205086